Chapter 10

Relativity for cyclists

Physicists like symmetry more than Nature
— Rich Kerswell

WHAT IF THE LAWS OF MOTION retain their form for a family of coordinate frames related by *continuous* symmetries? The notion of 'fundamental domain' is of no use here. If the symmetry is continuous, the dynamical system should be reduced to a lower-dimensional, desymmetrized system, with 'ignorable' coordinates eliminated (but not forgotten).

We shall describe here two ways of reducing a continuous symmetry. In the 'method of slices' or 'moving frames' of sect. 10.4 we slice the state space in such a way that an entire class of symmetry-equivalent points is represented by a single point. In the Hilbert polynomial basis approach of sect. 10.5 we replace the equivariant dynamics by the dynamics rewritten in terms of invariant coordinates. In either approach we retain the option of computing in the original coordinates, and then, when done, projecting the solution onto the symmetry reduced state space.

Instead of writing yet another tome on group theory, in what follows we continue to serve group theoretic nuggets on need-to-know basis, through a series of pedestrian examples (but take a slightly higher, cyclist road in the text proper).

10.1 Continuous symmetries

First of all, why worry about continuous symmetries? Here is an example of the effect a continuous symmetry has on dynamics (for physics background, see remark 10.2). exercise 10.1 exercise 10.8

Example 10.1 ***Complex Lorenz flow:*** *Consider a complex generalization of Lorenz*

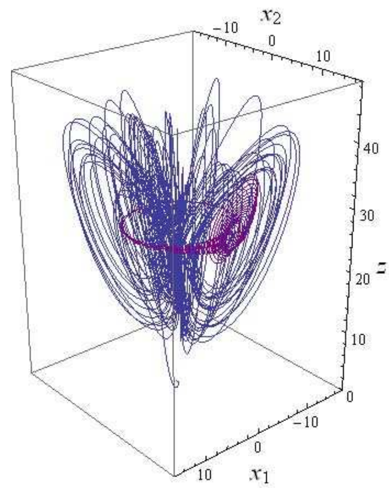

Figure 10.1: A typical $\{x_1, x_2, z\}$ trajectory of the complex Lorenz flow, with a short trajectory of figure 10.4 whose initial point is close to the relative equilibrium TW_1 superimposed. See also figure 10.7. (R. Wilczak)

equations (2.12),

$$\begin{aligned} \dot{x} &= -\sigma x + \sigma y\,, \qquad \dot{y} \;=\; (\rho - z)x - ay \\ \dot{z} &= (xy^* + x^*y)/2 - bz\,, \end{aligned} \tag{10.1}$$

where x, y are complex variables, z is real, while the parameters σ, b are real and $\rho = \rho_1 + i\rho_2$, $a = 1 - ie$ are complex. Recast in real variables, this is a set of five coupled ODEs

$$\begin{aligned} \dot{x}_1 &= -\sigma x_1 + \sigma y_1 \\ \dot{x}_2 &= -\sigma x_2 + \sigma y_2 \\ \dot{y}_1 &= (\rho_1 - z)x_1 - \rho_2 x_2 - y_1 - e y_2 \\ \dot{y}_2 &= \rho_2 x_1 + (\rho_1 - z)x_2 + e y_1 - y_2 \\ \dot{z} &= -bz + x_1 y_1 + x_2 y_2\,. \end{aligned} \tag{10.2}$$

In all numerical examples that follow, the parameters will be set to $\rho_1 = 28$, $\rho_2 = 0$, $b = 8/3$, $\sigma = 10$, $e = 1/10$, unless explicitly stated otherwise. As we shall show in example 10.7, this is a dynamical system with a continuous $SO(2)$ (but no discrete) symmetry.

Figure 10.1 offers a visualization of its typical long-time dynamics. What is wrong with this picture? It is a mess. As we shall show here, the attractor is built up by a nice 'stretch & fold' action, but that is totally hidden from the view by the continuous symmetry induced drifts. In the rest of this chapter we shall investigate various ways of 'quotienting' this $SO(2)$ symmetry, and reducing the dynamics to a 4-dimensional reduced state space. We shall not rest until we attain the simplicity of figure 10.12, and the bliss of the 1-dimensional return map of figure 10.14.

We shall refer to the component of the dynamics along the continuous symmetry directions as a 'drift.' In a presence of a continuous symmetry an orbit explores the manifold swept by combined action of the dynamics and the symmetry induced drifts. Further problems arise when we try to determine whether an orbit shadows another orbit (see the figure 13.1 for a sketch of a close pass to a periodic orbit), or develop symbolic dynamics (partition the state space, as in chapter 11): here a 1-dimensional trajectory is replaced by a $(N+1)$-dimensional 'sausage,' a dimension for each continuous symmetry (N being the total number of parameters specifying the continuous transformation, and '1' for the time parameter t). How are we to measure distances between such objects? In this chapter we shall learn here how to develop more illuminating visualizations of such flow than figure 10.1, 'quotient' symmetries, and offer computationally straightforward methods of reducing the dynamics to lower-dimensional, reduced state spaces. The methods should also be applicable to high-dimensional flows, such as translationally invariant fluid flows bounded by pipes or planes (see example 10.4).

But first, a lightning review of the theory of Lie groups. The group-theoretical concepts of sect. 9.1 apply to compact continuous groups as well, and will not be repeated here. All the group theory that we shall need is in principle contained in the *Peter-Weyl theorem*, and its corollaries: A compact Lie group G is completely reducible, its representations are fully reducible, every compact Lie group is a closed subgroup of a unitary group $U(n)$ for some n, and every continuous, unitary, irreducible representation of a compact Lie group is finite dimensional.

Example 10.2 ***Special orthogonal group SO(2)*** *(or S^1) is a group of length-preserving rotations in a plane. 'Special' refers to requirement that* $\det g = 1$*, in contradistinction to the orthogonal group* $O(n)$ *which allows for* $\det g = \pm 1$*. A group element can be parameterized by angle ϕ, with the group multiplication law $g(\phi')g(\phi) = g(\phi' + \phi)$, and its action on smooth periodic functions $u(\phi + 2\pi) = u(\phi)$ generated by*

$$g(\phi') = e^{\phi'\mathbf{T}} , \quad \mathbf{T} = \frac{d}{d\phi} . \tag{10.3}$$

Expand the exponential, apply it to a differentiable function $u(\phi)$, and you will recognize a Taylor series. So $g(\phi')$ shifts the coordinate by ϕ', $g(\phi')\, u(\phi) = u(\phi' + \phi)$.

exercise **??**

Example 10.3 ***Translation group:*** *Differential operator $\mathbf{T}$ in (10.3) is reminiscent of the generator of spatial translations. The 'constant velocity field' $v(x) = v = c \cdot \mathbf{T}$' acts on x_j by replacing it by the velocity vector c_j. It is easy to verify by Taylor expanding a function $u(x)$ that the time evolution is nothing but a coordinate translation by (time$\times$ velocity):*

$$e^{-\tau c\cdot\mathbf{T}}u(x) = e^{-\tau c\cdot\frac{d}{dx}}u(x) = u(x - \tau\, c) . \tag{10.4}$$

As x is a point in the Euclidean $\mathbb{R}^d$ space, the group is not compact. In general, a sequence of time steps in time evolution always forms an abelian Lie group, albeit *never as trivial as this free ballistic motion.*

If the group actions consist of N rotations which commute, for example act on an N-dimensional cell with periodic boundary conditions, the group is an abelian group that acts on a torus T^N.

Example 10.4 ***Continuous symmetries of the plane Couette flow.*** *(continued from example 9.7) The plane Couette flow is a Navier-Stokes flow bounded by two countermoving planes, in a cell periodic in streamwise and spanwise directions. Every solution of Navier-Stokes equations belongs, by the $SO(2) \times SO(2)$ symmetry, to a 2-torus T^2 of equivalent solutions. Furthermore these tori are interrelated by a discrete D_2 group of spanwise and streamwise flips of the flow cell. (continued in example 10.10)*

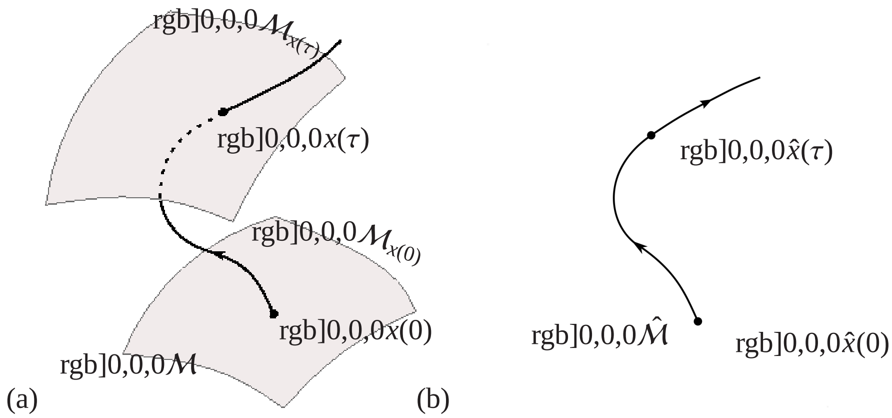

Figure 10.2: (a) The group orbit $\mathcal{M}_{x(0)}$ of state space point $x(0)$, and the group orbit $\mathcal{M}_{x(t)}$ reached by the trajectory $x(t)$ time t later. As any point on the manifold $\mathcal{M}_{x(t)}$ is physically equivalent to any other, the state space is foliated into the union of group orbits. (b) Symmetry reduction $\mathcal{M} \to \hat{\mathcal{M}}$ replaces each full state space group orbit $\mathcal{M}_x$ by a single point $\hat{x} \in \hat{\mathcal{M}}$.

Let G be a group, and $g\mathcal{M} \longrightarrow \mathcal{M}$ a group action on the state space $\mathcal{M}$. The $[d \times d]$ matrices g acting on vectors in the d-dimensional state space $\mathcal{M}$ form a linear representation of the group G. If the action of every element g of a group G commutes with the flow

$$g v(x) = v(gx)\,, \qquad g f^\tau(x) = f^\tau(gx)\,, \tag{10.5}$$

G is a symmetry of the dynamics, and, as in (9.7), the dynamics is said to be invariant under G, or *G-equivariant*.

In order to explore the implications of equivariance for the solutions of dynamical equations, we start by examining the way a compact Lie group acts on state space $\mathcal{M}$. For any $x \in \mathcal{M}$, the *group orbit* $\mathcal{M}_x$ of x is the set of all group actions (see page 162 and figure 10.2)

$$\mathcal{M}_x = \{g\, x \mid g \in G\}\,. \tag{10.6}$$

As we saw in example 10.3, the time evolution itself is a noncompact 1-parameter Lie group. Thus the time evolution and the continuous symmetries can be considered on the same Lie group footing. For a given state space point x a symmetry group of N continuous transformations together with the evolution in time sweeps out, in general, a smooth $(N{+}1)$-dimensional manifold of equivalent solutions (if the solution has a nontrivial symmetry, the manifold may have a dimension less than $N + 1$). For solutions p for which the group orbit of x_p is periodic in time T_p, the group orbit sweeps out a *compact* invariant manifold $\mathcal{M}_p$. The simplest example is the $N = 0$, no symmetry case, where the invariant manifold $\mathcal{M}_p$ is the 1-torus traced out by a periodic trajectory p. If $\mathcal{M}$ is a smooth C^∞ manifold, and G is compact and acts smoothly on $\mathcal{M}$, the reduced state space can be realized as a 'stratified manifold,' meaning that each group orbit (a 'stratum') is represented by a point in the reduced state space, see sect. 10.4. Generalizing the description of a non–wandering set of sect. 2.1.1, we say that for flows with continuous symmetries the non–wandering set Ω of dynamics (2.2) is the closure of the set of compact invariant manifolds $\mathcal{M}_p$. Without symmetries, we visualize the non–wandering set as a set of points; in presence of a continuous symmetry, each such 'point' is a group orbit.

10.1.1 Lie groups for pedestrians

> [...] which is an expression of consecration of 'angular momentum.'
>
> — Mason A. Porter's student

Definition: A Lie group is a topological group G such that (i) G has the structure of a smooth differential manifold, and (ii) the composition map $G \times G \to G$: $(g, h) \to gh^{-1}$ is smooth, i.e., $\mathbb{C}^\infty$ differentiable.

Do not be mystified by this definition. Mathematicians also have to make a living. Historically, the theory of compact Lie groups that we will deploy here emerged as a generalization of the theory of SO(2) rotations, i.e., Fourier analysis. By a 'smooth differential manifold' one means objects like the circle of angles that parameterize continuous rotations in a plane, example 10.2, or the manifold swept by the three Euler angles that parameterize SO(3) rotations.

An element of a compact Lie group continuously connected to identity can be written as

$$g(\phi) = e^{\phi\cdot\mathbf{T}}, \qquad \phi\cdot\mathbf{T} = \sum \phi_a \mathbf{T}_a,\ a = 1, 2, \cdots, N, \tag{10.7}$$

where $\phi \cdot \mathbf{T}$ is a *Lie algebra* element, and ϕ_a are the parameters of the transformation. Repeated indices are summed throughout this chapter, and the dot product refers to a sum over Lie algebra generators. The Euclidian product of two vectors x, y will be indicated by x-transpose times y, i.e., $x^T y = \sum_i^d x_i y_i$. Unitary transformations $\exp(\phi \cdot \mathbf{T})$ are generated by sequences of infinitesimal steps of form

$$g(\delta\phi) \simeq 1 + \delta\phi \cdot \mathbf{T}, \quad \delta\phi \in \mathbb{R}^N, \quad |\delta\phi| \ll 1, \tag{10.8}$$

where $\mathbf{T}_a$, the *generators* of infinitesimal transformations, are a set of linearly independent $[d\times d]$ anti-hermitian matrices, $(\mathbf{T}_a)^\dagger = -\mathbf{T}_a$, acting linearly on the d-dimensional state space $\mathcal{M}$. In order to streamline the exposition, we postpone discussion of combining continuous coordinate transformations with the discrete ones to sect. 10.2.1. . exercise 10.2

For continuous groups the Lie algebra, i.e., the set of N generators $\mathbf{T}_a$ of infinitesimal transformations, takes the role that the $|G|$ group elements play in the theory of discrete groups. The flow field at the state space point x induced by the action of the group is given by the set of N *tangent fields*

$$t_a(x)_i = (\mathbf{T}_a)_{ij} x_j, \tag{10.9}$$

which span the *tangent space*. Any representation of a compact Lie group G is fully reducible, and invariant tensors constructed by contractions of $\mathbf{T}_a$ are useful for identifying irreducible representations. The simplest such invariant is

$$\mathbf{T}^T \cdot \mathbf{T} = \sum_\alpha C_2^{(\alpha)} \ \mathbb{1}^{(\alpha)} , \tag{10.10}$$

where $C_2^{(\alpha)}$ is the quadratic Casimir for irreducible representation labeled α, and $\mathbb{1}^{(\alpha)}$ is the identity on the α-irreducible subspace, 0 elsewhere. The dot product of two tangent fields is thus a sum weighted by Casimirs,

$$t(x)^T \cdot t(x') = \sum_\alpha C_2^{(\alpha)} x_i \, \delta_{ij}^{(\alpha)} x'_j \, . \tag{10.11}$$

Example 10.5 ***SO*(2) *irreducible representations:*** *(continued from example 10.2) Expand a smooth periodic function $u(\phi + 2\pi) = u(\phi)$ as a Fourier series*

$$u(\phi) = a_0 + \sum_{m=1}^{\infty} (a_m \cos m\phi + b_m \sin m\phi) \ . \tag{10.12}$$

The matrix representation of the $SO(2)$ action (10.3) on the mth Fourier coefficient pair (a_m, b_m) is

$$g^{(m)}(\phi') \ = \left(\begin{array}{cc} \cos m\phi' & \sin m\phi' \\ -\sin m\phi' & \cos m\phi' \end{array} \right) , \tag{10.13}$$

with the Lie group generator

$$\mathbf{T}^{(m)} \ = \left(\begin{array}{cc} 0 & m \\ -m & 0 \end{array} \right) . \tag{10.14}$$

The $SO(2)$ group tangent (10.9) to state space point $u(\phi)$ on the mth invariant subspace is

$$t^{(m)}(u) \ = \ m \left(\begin{array}{c} b_m \\ -a_m \end{array} \right) . \tag{10.15}$$

The L^2 norm of $t(u)$ is weighted by the $SO(2)$ quadratic Casimir (10.10), $C_2^{(m)} = m^2$,

$$\oint \frac{d\phi}{2\pi} \, (\mathbf{T}u(\phi))^T \mathbf{T}u(2\pi - \phi) = \sum_{m=1}^{\infty} m^2 \left(a_m^2 + b_m^2\right) , \tag{10.16}$$

and converges only for sufficiently smooth $u(\phi)$. What does that mean? We saw in (10.4) that $\mathbf{T}$ generates translations, and by (10.14) the velocity of the mth Fourier mode is m times higher than for the $m = 1$ component. If $|u^{(m)}|$ does not fall off faster the $1/m$, the action of $SO(2)$ is overwhelmed by the high Fourier modes.

Example 10.6 ***SO*(2) rotations for complex Lorenz equations:** *Substituting the Lie algebra generator*

$$\mathbf{T} = \begin{pmatrix} 0 & 1 & 0 & 0 & 0 \\ -1 & 0 & 0 & 0 & 0 \\ 0 & 0 & 0 & 1 & 0 \\ 0 & 0 & -1 & 0 & 0 \\ 0 & 0 & 0 & 0 & 0 \end{pmatrix} \qquad (10.17)$$

acting on a 5-dimensional space (10.2) into (10.7) yields a finite angle $SO(2)$ rotation:

$$g(\phi) = \begin{pmatrix} \cos\phi & \sin\phi & 0 & 0 & 0 \\ -\sin\phi & \cos\phi & 0 & 0 & 0 \\ 0 & 0 & \cos\phi & \sin\phi & 0 \\ 0 & 0 & -\sin\phi & \cos\phi & 0 \\ 0 & 0 & 0 & 0 & 1 \end{pmatrix}. \qquad (10.18)$$

From (10.13) we see that the action of $SO(2)$ on the complex Lorenz equations state space decomposes into $m = 0$ G-invariant subspace (z-axis) and $m = 1$ subspace with multiplicity 2.

The generator $\mathbf{T}$ is indeed anti-hermitian, $\mathbf{T}^\dagger = -\mathbf{T}$, and the group is compact, its elements parametrized by ϕ mod 2π. Locally, at $x \in \mathcal{M}$, the infinitesimal action of the group is given by the group tangent field $t(x) = \mathbf{T}x = (x_2, -x_1, y_2, -y_1, 0)$. In other words, the flow induced by the group action is normal to the radial direction in the (x_1, x_2) and (y_1, y_2) planes, while the z-axis is left invariant.

fast track:
sect. 10.2, p. 189

10.1.2 Lie groups for cyclists

appendix A.2.3

> Henriette Roux: "Why do you devote to Lie groups only a page, while only a book-length monograph can do it justice?" A: "ChaosBook tries its utmost to minimize the Gruppenpest jargon damage, which is a total turnoff to our intended audience of working plumbers and electricians. The sufferings of our master plumber Fabian Waleffe while reading chapter 9 - World in a mirror are chicken feed in comparison to the continuous symmetry reduction nightmare that we embark upon here."
>
> —

Here comes all of the theory of Lie groups in one quick serving. You will live even if you do not digest this section, or, to spell it out; skip this section unless you already know the theory of Lie algebras.

The $[d\times d]$ matrices g acting on vectors in the state space $\mathcal{M}$ form a linear representation of the group G. Tensors transform as

$$h'_{ij}{}^{k} = g_i{}^{i'} g_j{}^{j'} g^k{}_{k'} h_{i'j'}{}^{k'} . \qquad (10.19)$$

A multilinear function $h(\overline{q}, \overline{r}, \ldots, s)$ is an invariant function if (and only if) for any transformation $g \in G$ and for any set of vectors $q, r, s, \ldots$ it is unchanged by the coordinate transformation

$$h(\overline{gq}, \overline{gr}, \ldots gs) = h(\overline{q}, \overline{r}, \ldots, s) = h_{ab\cdots}{}^{\cdots c}\, q^a r^b \cdots s_c\,. \tag{10.20}$$

Examples of such invariant functions are the length $r(x)^2 = \delta_i^j x^i x_j$ and the volume $V(x, y, z) = \epsilon^{ijk} x_i y_j z_k$. Substitute the infinitesimal form of group action (10.8) into (10.19), keep the linear terms. In the index-notation longhand, the Lie algebra generator acts on each index separately,

$$(\mathbf{T}_a)_i^{i'} h_{i' j\ldots}{}^{k\ldots} + (\mathbf{T}_a)_j^{j'} h_{i j'\ldots}{}^{k\ldots} - (\mathbf{T}_a)_{k'}^{k} h_{i j\ldots}{}^{k'\ldots} + \ldots = 0\,. \tag{10.21}$$

Hence the tensor $h_{ij\ldots}{}^{\ldots k}$ is invariant if $\mathbf{T}_a h = 0$, i.e., the N generators $\mathbf{T}_a$ 'annihilate' it.

As one does not want the symmetry rules to change at every step, the generators $\mathbf{T}_a$, $a = 1, 2, \ldots, N$, are themselves invariant tensors:

$$(\mathbf{T}_a)\,{}_j^{\,i} = g^i{}_{i'}\, g_j{}^{j'}\, g_{aa'}\, (\mathbf{T}_{a'})\,{}_{j'}^{\,i'}\,, \tag{10.22}$$

where $g_{ab} = \left[e^{-i\phi\cdot C}\right]_{ab}$ is the adjoint $[N\times N]$ matrix representation of $g \in G$. The $[d\times d]$ matrices $\mathbf{T}_a$ are in general non-commuting, and from (10.21) it follows that they close N-element *Lie algebra*

$$[\mathbf{T}_a, \mathbf{T}_b] = \mathbf{T}_a\mathbf{T}_b - \mathbf{T}_b\mathbf{T}_a = -C_{abc}\mathbf{T}_c\,, \qquad a, b, c = 1, 2, ..., N\,,$$

where the fully antisymmetric adjoint representation hermitian generators

$$[C_c]_{ab} = C_{abc} = -C_{bac} = -C_{acb}$$

are the *structure constants* of the Lie algebra.

As we will not use non-abelian Lie groups in this chapter, we omit the derivation of the Jacobi relation between C_{abc}'s, and you can safely ignore all this talk of tensors and Lie algebra commutators as far as the pedestrian applications at hand are concerned.

10.1.3 Equivariance under infinitesimal transformations

A flow $\dot{x} = v(x)$ is G-equivariant (10.5) if

exercise 10.4
exercise 10.5

$$v(x) = g^{-1}\, v(g\, x)\,, \qquad \text{for all } g \in G\,. \tag{10.23}$$

For an infinitesimal transformation (10.8) the G-equivariance condition becomes

$$v(x) = (1 - \phi \cdot \mathbf{T})\, v(x + \phi \cdot \mathbf{T}x) + \cdots = v(x) - \phi \cdot \mathbf{T}v(x) + \frac{dv}{dx}\,\phi \cdot \mathbf{T}x + \cdots\,.$$

The $v(x)$ cancel, and ϕ_a are arbitrary. Denote the *group flow tangent field* at x by $t_a(x)_i = (\mathbf{T}_a)_{ij} x_j$. Thus the infinitesimal, Lie algebra G-equivariance condition is

$$t_a(v) - A(x)\, t_a(x) = 0\,, \tag{10.24}$$

where $A = \partial v/\partial x$ is the stability matrix (4.3). If case you find such learned remarks helpful: the left-hand side of (10.24) is the *Lie derivative* of the dynamical flow field v along the direction of the infinitesimal group-rotation induced flow $t_a(x) = \mathbf{T}_a x$,

$$\mathcal{L}_{t_a} v = \left(\mathbf{T}_a - \frac{\partial}{\partial y}(\mathbf{T}_a x)\right) v(y)\Big|_{y=x}\,. \tag{10.25}$$

exercise 10.6
exercise 10.7
exercise 10.12

The equivariance condition (10.24) states that the two flows, one induced by the dynamical vector field v, and the other by the group tangent field t, commute if their Lie derivatives (or the 'Lie brackets ' or 'Poisson brackets') vanish.

Example 10.7 ***Equivariance of complex Lorenz flow:*** *That complex Lorenz flow (10.2) is equivariant under $SO(2)$ rotations (10.18) can be checked by substituting the Lie algebra generator (10.17) and the stability matrix (4.3) for complex Lorenz flow (10.2),*

$$A = \begin{pmatrix} -\sigma & 0 & \sigma & 0 & 0 \\ 0 & -\sigma & 0 & \sigma & 0 \\ \rho_1 - z & -\rho_2 & -1 & -e & -x_1 \\ \rho_2 & \rho_1 - z & e & -1 & -x_2 \\ y_1 & y_2 & x_1 & x_2 & -b \end{pmatrix}, \tag{10.26}$$

into the equivariance condition (10.24). Considering that $t(v)$ depends on the full set of equations (10.2), and $A(x)$ is only its linearization, this is not an entirely trivial statement. For the parameter values (10.2) the flow is strongly volume contracting (4.42),

$$\partial_i v_i = \sum_{i=1}^{5} \lambda_i(x,t) = -b - 2(\sigma + 1) = -24 - 2/3\,, \tag{10.27}$$

at a coordinate-, ρ- and e-independent constant rate.

Checking equivariance as a Lie algebra condition (10.24) is easier than checking it for global, finite angle rotations (10.23).

10.2 Symmetries of solutions

Let $v(x)$ be the dynamical flow, and f^τ the trajectory or 'time-τ forward map' of an initial point x_0,

$$\frac{dx}{dt} = v(x) , \qquad x(\tau) = f^\tau(x_0) = x_0 + \int_0^\tau d\tau'\, v(x(\tau')) . \tag{10.28}$$

As discussed in sect. 9.2, solutions $x(\tau)$ of an equivariant system can satisfy all of the system's symmetries, a subgroup of them, or have no symmetry at all. For a given solution $x(\tau)$, the subgroup that contains all symmetries that fix x (that satisfy $gx = x$) is called the isotropy (or stabilizer) subgroup of x. A generic ergodic trajectory $x(\tau)$ has no symmetry beyond the identity, so its isotropy group is $\{e\}$, but recurrent solutions often do. At the other extreme is equilibrium, whose isotropy group is the full symmetry group G.

The simplest solutions are the *equilibria* or *steady* solutions (2.8).

Definition: Equilibrium $x_{EQ} = \mathcal{M}_{EQ}$ is a fixed, time-invariant solution,

$$\begin{aligned} v(x_{EQ}) &= 0 , \\ x(x_{EQ}, \tau) &= x_{EQ} + \int_0^\tau d\tau'\, v(x(\tau')) = x_{EQ} . \end{aligned} \tag{10.29}$$

An *equilibrium* with full symmetry,

$$g\, x_{EQ} = x_{EQ} \qquad \text{for all } g \in G ,$$

lies, by definition, in Fix (G) subspace (**??**), for example the x_3 axis in figure 10.3 (a). The multiplicity of such solution is one. An equilibrium x_{EQ} with symmetry G_{EQ} smaller than the full group G belongs to a group orbit G/G_{EQ}. If G is finite there are $|G|/|G_{EQ}|$ equilibria in the group orbit, and if G is continuous then the group orbit of x is a continuous family of equilibria of dimension $\dim G - \dim G_{EQ}$. For example, if the angular velocity c in figure 10.3 (b) equals zero, the group orbit consists of a circle of (dynamically static) equivalent equilibria.

exercise 10.13
exercise 10.14

Definition: Relative equilibrium solution $x_{TW}(\tau) \in \mathcal{M}_{TW}$: the dynamical flow field points along the group tangent field, with constant 'angular' velocity c, and the trajectory stays on the group orbit, see figure 10.3 (a):

exercise 10.17
exercise 10.19
exercise 10.20
exercise 10.21
exercise 10.22
exercise 10.26
exercise 10.27

$$\begin{aligned} v(x) &= c \cdot t(x) , \qquad x \in \mathcal{M}_{TW} \\ x(\tau) &= g(-\tau\, c)\, x(0) \;=\; e^{-\tau\, c\cdot \mathbf{T}} x(0) . \end{aligned} \tag{10.30}$$

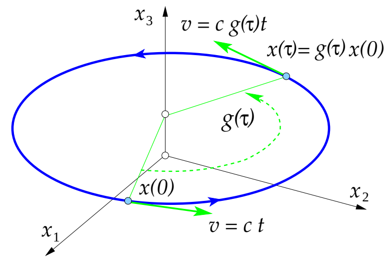

Figure 10.3: (a) A *relative equilibrium orbit* starts out at some point $x(0)$, with the dynamical flow field $v(x) = c \cdot t(x)$ pointing along the group tangent space. For the SO(2) symmetry depicted here, the flow traces out the group orbit of $x(0)$ in time $T = 2\pi/c$. (b) An *equilibrium* lives either in the fixed Fix (G) subspace (x_3 axis in this sketch), or on a group orbit as the one depicted here, but with zero angular velocity c. In that case the circle (in general, N-torus) depicts a continuous family of fixed equilibria, related only by the group action.

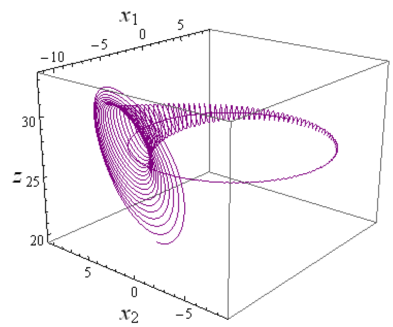

Figure 10.4: $\{x_1, x_2, z\}$ plot of the complex Lorenz flow with initial point close to TW_1. In figure 10.1 this relative equilibrium is superimposed over the strange attractor. (R. Wilczak)

A *traveling wave* remark 10.3

$$x(\tau) = g(-c\tau)\, x_{TW} = x_{TW} - c\,\tau\,, \qquad c \in \mathbb{R}^d \tag{10.31}$$

is a special type of a relative equilibrium of equivariant evolution equations, where the action is given by translation (10.4), $g(y)\, x(0) = x(0) + y$. A *rotating wave* is another special case of relative equilibrium, with the action is given by angular rotation. By equivariance, all points on the group orbit are equivalent, the magnitude of the velocity c is same everywhere along the orbit, so a 'traveling wave' moves at a constant speed. For an $N > 1$ trajectory traces out a line within the group orbit. As the c_a components are generically not in rational ratios, the trajectory explores the N-dimensional group orbit (10.6) quasi-periodically. In other words, the group orbit $g(\tau)\, x(0)$ coincides with the dynamical orbit $x(\tau) \in \mathcal{M}_{TW}$ and is thus flow invariant.

Example 10.8 ***A relative equilibrium:*** *For complex Lorenz equations and our canonical parameter values of (10.2) a computation yields the relative equilibrium TW_1 with a representative group orbit point*

$$(x_1, x_2, y_1, 0, z)_{TW1} = (8.48492, 0.0771356, 8.48562, 0, 26.9999)\,, \tag{10.32}$$

and angular velocity $c_{TW1} = 1/11$. This corresponds to period $T_{TW1} = 2\pi/c \approx 69$, so a simulation has to be run up to time of order of at least 70 for the strange attractor in figure 10.1 to start filling in.

Figure 10.4 shows the complex Lorenz flow with the initial point (10.32) on the relative equilibrium TW_1. It starts out by drifting in a circle around the z-axis, but as the numerical errors accumulate, the trajectory spirals out.

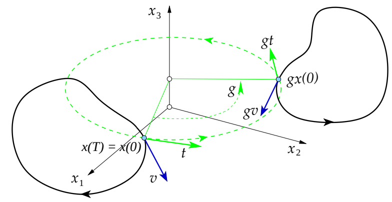

Figure 10.5: A periodic orbit starts out at $x(0)$ with the dynamical v and group tangent t flows pointing in different directions, and returns after time T_p to the initial point $x(0) = x(T_p)$. The group orbit of the temporal orbit of $x(0)$ sweeps out a $(1+N)$-dimensional torus, a continuous family of equivalent periodic orbits, two of which are sketched here. For SO(2) this is topologically a 2-torus.

Calculation of the relative equilibrium stability reveals that it is spiral-out unstable, with the very short period $T_{spiral} = 0.6163$. *This is the typical time scale for fast oscillations visible in figure 10.1, with some 100 turns for one circumambulation of the* TW_1 *orbit. In that time an initial deviation from* x_{TW1} *is multiplied by the factor* $\Lambda_{radial} \approx 500$. *It would be sweet if we could eliminate the drift time scale* ≈ 70 *and focus just on the fast time scale of* ≈ 0.6. *That we will attain by reformulating the dynamics in a reduced state space.*

Definition: Periodic orbit. Let x be a periodic point on the periodic orbit p of period T,

$$f^T(x) = x\,, \qquad x \in \mathcal{M}_p.$$

By equivariance, $g\,x$ is another periodic point, with the orbits of x and gx either identical or disjoint.

If gx lands on the same orbit, g is an element of periodic orbit's symmetry group G_p. If the symmetry group is the full group G, we are back to (10.30), i.e., the periodic orbit is the group orbit traced out by a relative equilibrium. The other option is that the isotropy group is discrete, the orbit segment $\{x, gx\}$ is pre-periodic (or eventually periodic), $x(0) = g_p x(T_p)$, where T_p is a fraction of the full period, $T_p = T/m$, and thus

$$\begin{aligned} x(0) &= g_p x(T_p)\,, \qquad x \in \mathcal{M}_p\,, \qquad g_p \in G_p \\ x(0) &= g_p^m x(m\,T_p) = x(T) = x(0)\,. \end{aligned} \tag{10.33}$$

If the periodic solutions are disjoint, as in figure 10.5, their multiplicity (if G is finite, see sect. 9.1), or the dimension of the manifold swept under the group action (if G is continuous) can be determined by applications of $g \in G$. They form a family of conjugate solutions (9.19),

$$\mathcal{M}_{g\,p} = g\,\mathcal{M}_p\,g^{-1}\,. \tag{10.34}$$

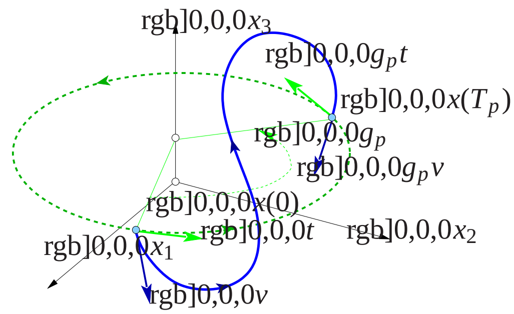

Figure 10.6: A relative periodic orbit starts out at $x(0)$ with the dynamical v and group tangent t flows pointing in different directions, and returns to the group orbit of $x(0)$ after time T_p at $x(T_p) = g_p x(0)$, a rotation of the initial point by g_p. For flows with continuous symmetry a generic relative periodic orbit (not pre-periodic to a periodic orbit) fills out ergodically what is topologically a torus, as in figure 10.5; if you are able to draw such a thing, kindly send us the figure. As illustrated by figure 10.8 (a) this might be a project for Lucas Films.

Definition: Relative periodic orbit p is an orbit $\mathcal{M}_p$ in state space $\mathcal{M}$ which exactly recurs

$$x_p(0) = g_p x_p(T_p)\,, \qquad x_p(\tau) \in \mathcal{M}_p\,, \tag{10.35}$$

at a fixed *relative period* T_p, but shifted by a fixed group action g_p which brings the endpoint $x_p(T_p)$ back into the initial point $x_p(0)$, see figure 10.6. The group action g_p parameters $\phi = (\phi_1, \phi_2, \cdots \phi_N)$ are referred to as "phases," or "shifts." In contrast to the pre-periodic (10.33), the phase here are irrational, and the trajectory sweeps out ergodically the group orbit without ever closing into a periodic orbit. For dynamical systems with only continuous (no discrete) symmetries, the parameters $\{t, \phi_1, \cdots, \phi_N\}$ are real numbers, ratios π/ϕ_j are almost never rational, likelihood of finding a periodic orbit for such system is zero, and such relative periodic orbits are almost never eventually periodic.

Relative periodic orbits are to periodic solutions what relative equilibria (traveling waves) are to equilibria (steady solutions). Equilibria satisfy $f^\tau(x) - x = 0$ and relative equilibria satisfy $f^\tau(x) - g(\tau)\, x = 0$ for any τ. In a co-moving frame, i.e., frame moving along the group orbit with velocity $v(x) = c \cdot t(x)$, the relative equilibrium appears as an equilibrium. Similarly, a relative periodic orbit is periodic in its mean velocity $c_p = \phi_p/T_p$ co-moving frame (see figure 10.8), but in the stationary frame its trajectory is quasiperiodic. A co-moving frame is helpful in visualizing a single 'relative' orbit, but useless for viewing collections of orbits, as each one drifts with its own angular velocity. Visualization of all relative periodic orbits as periodic orbits we attain only by global symmetry reductions, to be undertaken in sect. 10.4.

Example 10.9 ***Complex Lorenz flow with relative periodic orbit:*** *Figure 10.7 is a group portrait of the complex Lorenz equations state space dynamics, with several important players posing against a generic orbit in the background.*

The unstable manifold of relative equilibrium TW_1 is characterized by a 2-dimensional complex eigenvector pair, so its group orbit is a 3-dimensional. Only one representative trajectory on it is plotted in the figure. The unstable manifold of equilibrium EQ_0 has one expanding eigenvalue, but its group orbit is a cone originating at EQ_0. Only one representative trajectory on this cone is shown in the figure. It lands close to TW_1, and then spirals out along its unstable manifold. 3 repetitions of a short relative periodic orbit $\overline{01}$ are drawn. The trajectory fills out ergodically a 2-dimensional

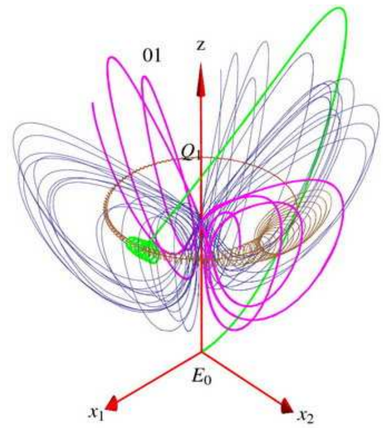

Figure 10.7: (Figure 10.1 continued) A group portrait of the complex Lorenz equations state space dynamics. Plotted are relative equilibrium TW_1 (red), its unstable manifold (brown), equilibrium EQ_0, one trajectory from the group orbit of its unstable manifold (green), 3 repetitions of relative periodic orbit $\overline{01}$ (magenta) and a generic orbit (blue). (E. Siminos)

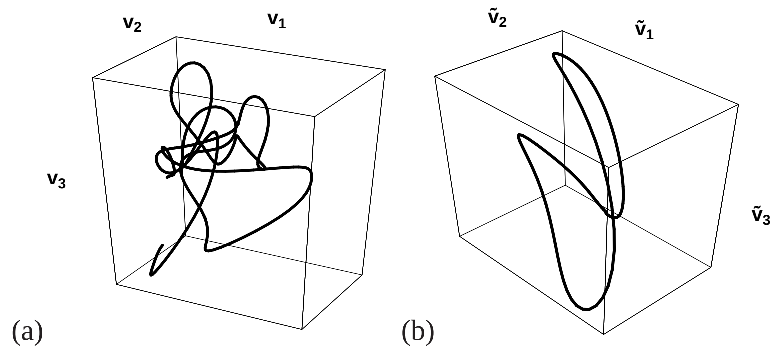

Figure 10.8: A relative periodic orbit of Kuramoto-Sivashinsky flow projected on (a) the stationary state space coordinate frame $\{v_1, v_2, v_3\}$, traced for four periods T_p; (b) the co-moving $\{\tilde{v}_1, \tilde{v}_2, \tilde{v}_3\}$ coordinate frame, moving with the mean angular velocity $c_p = \phi_p/T_p$. (from ref. [10.1])

orbit $\mathcal{M}_{01}$. The assignment of its symbolic dynamics label will be possible only after the symmetry reduction, see figure 10.14 and figure 11.9.

10.2.1 Discrete and continuous symmetries together

We expect to see relative periodic orbits because a trajectory that starts on and returns to a given torus of a symmetry equivalent solutions is unlikely to intersect it at the initial point, unless forced to do so by a discrete symmetry. This we will make explicit in sect. 10.4, where relative periodic orbits will be viewed as periodic orbits of the reduced dynamics.

If, in addition to a continuous symmetry, one has a discrete symmetry which is not its subgroup, one does expect equilibria and periodic orbits. However, a relative periodic orbit can be pre-periodic if it is equivariant under a discrete symmetry, as in (10.33): If $g^m = 1$ is of finite order m, then the corresponding orbit is periodic with period mT_p. If g is not of a finite order, a relative periodic orbit is periodic only after a shift by g_p, as in (10.35). Morally, as it will be shown in chapter 21, such orbit is the true 'prime' orbit, i.e., the shortest segment that under action of G tiles the entire invariant submanifold $\mathcal{M}_p$.

Definition: Relative orbit $\mathcal{M}_{Gx}$ in state space $\mathcal{M}$ is the time evolved *group orbit* $\mathcal{M}_x$ of a state space point x, the set of all points that can be reached from x

by all symmetry group actions and evolution of each in time.

$$\mathcal{M}_{x(t)} = \{gxt : t \in \mathbb{R}, g \in G\} \,. \tag{10.36}$$

In presence of symmetry, an equilibrium is the set of all equilibria related by symmetries, an relative periodic orbit is the hyper-surface traced by a trajectory in time T and all group actions, etc..

Example 10.10 ***Relative orbits in the plane Couette flow.*** *(continued from example 10.4)* *Translational symmetry allows for relative equilibria (traveling waves), characterized by a fixed profile Eulerian velocity $u_{TW}(x)$ moving with constant velocity c, i.e.*

$$u(x, \tau) = u_{TW}(x - c\tau) \,. \tag{10.37}$$

As the plane Couette flow is bounded by two counter-moving planes, it is easy to see where the relative equilibrium (traveling wave) solutions come from. A relative equilibrium solution hugs close to one of the walls and drifts with it with constant velocity, slower than the wall, while maintaining its shape. A relative periodic solution is a solution that recurs at time T_p with exactly the same disposition of the Eulerian velocity fields over the entire cell, but shifted by a 2-dimensional (streamwise,spanwise) translation g_p. By discrete symmetries these solutions come in counter-traveling pairs $u_q(x - c\tau)$, $-u_q(-x + c\tau)$: for example, for each one drifting along with the upper wall, there is a counter-moving one drifting along with the lower wall. Discrete symmetries also imply existence of strictly stationary solutions, or 'standing waves.' For example, a solution with velocity fields antisymmetric under reflection through the midplane has equal flow velocities in opposite directions, and is thus an equilibrium stationary in time.

chapter 21

10.3 Stability

A spatial derivative of the equivariance condition (10.5) yields the matrix equivariance condition satisfied by the stability matrix (stated here both for the finite group actions, and for the infinitesimal, Lie algebra generators):

exercise 10.28
exercise 10.29

$$gA(x)g^{-1} = A(gx) \,, \qquad [\mathbf{T}_a, A] = \frac{\partial A}{\partial x} t_a(x) \,. \tag{10.38}$$

For a flow within the fixed $\mathrm{Fix}\,(G)$ subspace, $t(x)$ vanishes, and the symmetry imposes strong conditions on the perturbations out of the $\mathrm{Fix}\,(G)$ subspace. As in this subspace stability matrix A commutes with the Lie algebra generators $\mathbf{T}$, the spectrum of its eigenvalues and eigenvectors is decomposed into irreducible representations of the symmetry group. This we have already observed for the EQ_0 of the Lorenz flow in example 9.14.

A infinitesimal symmetry group transformation maps the initial and the end point of a finite trajectory into a nearby, slightly rotated equivalent points, so we expect the perturbations along to group orbit to be marginal, with unit eigenvalues. The argument is akin to (4.7), the proof of marginality of perturbations along a periodic orbit. Consider two nearby initial points separated by an N-dimensional infinitesimal group transformation (10.8): $\delta x_0 = g(\delta\phi)x_0 - x_0 = \delta\phi \cdot \mathbf{T}x_0 = \delta\phi \cdot t(x_0)$. By the commutativity of the group with the flow, $g(\delta\phi)f^\tau(x_0) = f^\tau(g(\delta\phi)x_0)$. Expanding both sides, keeping the leading term in $\delta\phi$, and using the definition of the Jacobian matrix (4.6), we observe that $J^\tau(x_0)$ transports the N-dimensional group tangent space at $x(0)$ to the rotated tangent space at $x(\tau)$ at time τ:

$$t_a(\tau) = J^\tau(x_0)\, t_a(0)\,, \qquad t_a(\tau) = \mathbf{T}_a\, x(\tau)\,. \tag{10.39}$$

For a relative periodic orbit, $g_p x(T_p) = x(0)$, at any point along cycle p the group tangent vector $t_a(\tau)$ is an eigenvector of the Jacobian matrix with an eigenvalue of unit magnitude,

$$J_p\, t_a(x) = t_a(x)\,, \qquad J_p(x) = g_p J^{T_p}(x)\,, \qquad x \in \mathcal{M}_p\,. \tag{10.40}$$

Two successive points along the cycle separated by $\delta x_0 = \delta\phi \cdot t(\tau)$ have the same separation after a completed period $\delta x(T_p) = g_p \delta x_0$, hence eigenvalue of magnitude 1. In presence of an N-dimensional Lie symmetry group, N eigenvalues equal unity.

10.4 Reduced state space

> Maybe when I'm done with grad school I'll be able to figure it all out . . .
>
> — Rebecca Wilczak, undergraduate

Given Lie group G acting smoothly on a C^∞ manifold $\mathcal{M}$, we can think of each group orbit as an equivalence class. *Symmetry reduction* is the identification of a unique point on a group orbit as the representative of its equivalence class. We call the set of all such group orbit representatives the *reduced state space* $\mathcal{M}/G$. In the literature this space is often rediscovered, and thus has many names - it is alternatively called 'desymmetrized state space,' 'symmetry-reduced space,' 'orbit space' (because every group orbit in the original space is mapped to a single point in the orbit space), or 'quotient space' (because the symmetry has been 'divided out'), obtained by mapping equivariant dynamics to invariant dynamics ('image') by methods such as 'moving frames,' 'cross sections,' 'slices,' 'freezing,' 'Hilbert bases,' 'quotienting,' 'lowering of the degree,' 'lowering the order,' or 'desymmetrization.' remark 10.1

Symmetry reduction replaces a dynamical system $(\mathcal{M}, f)$ with a symmetry by a 'desymmetrized' system $(\hat{\mathcal{M}}, \bar{f})$, a system where each group orbit is replaced by a point, and the action of the group is trivial, $g\hat{x} = \hat{x}$ for all $\hat{x} \in \hat{\mathcal{M}}$, $g \in G$. The reduced state space $\hat{\mathcal{M}}$ is sometimes called the 'quotient space' $\mathcal{M}/G$ because

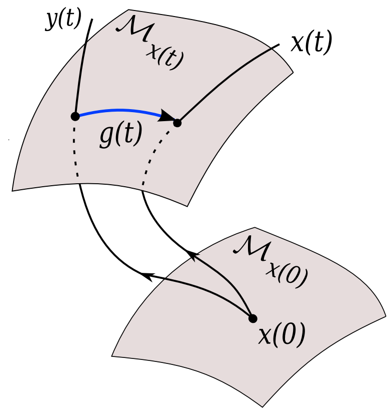

Figure 10.9: A point x on the full state space trajectory $x(t)$ is equivalent up to a group rotation $g(t)$ to the point $\hat{x}$ on the curve $\hat{x}(t)$ if the two points belong to the same group orbit $\mathcal{M}_x$, see (10.6).

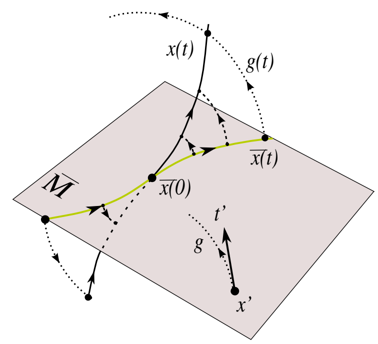

Figure 10.10: Slice $\hat{\mathcal{M}}$ is a hyperplane (10.42) passing through the slice-fixing point $\hat{x}'$, and normal to the group tangent t' at $\hat{x}'$. It intersects all group orbits (indicated by dotted lines here) in an open neighborhood of $\hat{x}'$. The full state space trajectory $x(\tau)$ and the reduced state space trajectory $\hat{x}(\tau)$ belong to the same group orbit $\mathcal{M}_{x(\tau)}$ and are equivalent up to a group rotation $g(\tau)$, defined in (10.41).

the symmetry has been 'divided out.' For a discrete symmetry, the reduced state space $\mathcal{M}/G$ is given by the fundamental domain of sect. 9.4. In presence of a continuous symmetry, the reduction to $\mathcal{M}/G$ amounts to a change of coordinates where the 'ignorable angles' $\{\phi_1, \cdots, \phi_N\}$ that parameterize N group translations can be separated out.

We start our discussion of symmetry reduction by considering the finite-rotations *method of moving frames*, and its differential formulation, the *method of slices*.

10.4.1 Go with the flow: method of moving frames

The idea: We can, at least locally, map each point along any solution $x(\tau)$ to the unique representative $\hat{x}(\tau)$ of the associated group orbit equivalence class, by a suitable rotation

$$x(\tau) = g(\tau)\,\hat{x}(\tau)\,. \tag{10.41}$$

Equivariance implies the two points are equivalent. In the 'method of slices' the reduced state space representative $\hat{x}$ of a group orbit equivalence class is picked by slicing across the group orbits by a fixed hypersurface. We start by describing how the method works for a finite segment of the full state space trajectory.

Definition: Slice. Let G act regularly on a d-dimensional manifold $\mathcal{M}$, i.e., with all group orbits N-dimensional. A *slice* through point $\hat{x}'$ is a $(d-N)$-dimensional submanifold $\hat{\mathcal{M}}$ such that all group orbits in an open neighborhood of the slice-defining point $\hat{x}'$ intersect $\hat{\mathcal{M}}$ transversally and only once (see figure 10.10).

The simplest *slice condition* defines a linear slice as a $(d-N)$-dimensional hyperplane $\hat{\mathcal{M}}$ normal to the N group rotation tangents t'_a at point $\hat{x}'$:

$$(\hat{x} - \hat{x}')^T t'_a = 0\,, \qquad t'_a = t_a(\hat{x}') = \mathbf{T}_a\,\hat{x}'\,. \tag{10.42}$$

In other words, 'slice' is a Poincaré section (3.6) for group orbits. Each 'big circle' –group orbit tangent to t'_a– intersects the hyperplane exactly twice, with the two solutions separated by π. As for a Poincaré section (3.4), we add an orientation condition, and select the intersection with the clockwise rotation angle into the slice.

Definition: Moving frame. Assume that for a given $x \in \mathcal{M}$ and a given slice $\hat{\mathcal{M}}$ there exists a unique group element $g = g(x)$ that rotates x into the slice, $gx = \hat{x} \in \hat{\mathcal{M}}$. The map that associates to a state space point x a Lie group action $g(x)$ is called a *moving frame*.

exercise 6.1
exercise 10.30

As $(\hat{x}')^T t'_a = 0$ by the antisymmetry of $\mathbf{T}_a$, the slice condition (10.42) fixes ϕ for a given x by

$$0 = \hat{x}^T t'_a = x^T g(\phi)^T t'_a\,, \tag{10.43}$$

where g^T denotes the transpose of g. The method of moving frames can be interpreted as a change of variables

$$\hat{x}(\tau) = g^{-1}(\tau)\,x(\tau)\,, \tag{10.44}$$

that is passing to a frame of reference in which condition (10.43) is identically satisfied, see example 10.11. Therefore the name 'moving frame.' Method of moving frames should not be confused with the co-moving frames, such as the one illustrated in figure 10.8. Each relative periodic orbit has its own co-moving frame. In the method of moving frames (or the method of slices) one fixes a stationary slice, and rotates all solutions back into the slice.

The method of moving frames is a post-processing method; trajectories are computed in the full state space, then rotated into the slice whenever desired, with the slice condition easily implemented. The slice group tangent t' is a given vector, and $g(\phi)\,x$ is another vector, linear in x and a function of group parameters ϕ. Rotation parameters ϕ are determined numerically, by a Newton method, through the slice condition (10.43).

Figure 10.11 illustrates the method of moving frames for an SO(2) slice normal to the x_2 axis. Looks innocent, except there is nothing to prevent a trajectory from going through $(x_1, x_2) = (0, 0)$, and what ϕ is one to use then? We can always chose a finite time step that hops over this singularity, but in the continuous time formulation we will not be so lucky.

How does one pick a slice point $\hat{x}'$? A generic point $\hat{x}'$ not in an invariant subspace (on the complex Lorenz equations z axis, for example) should suffice to fix a slice. The rules of thumb are much like the ones for picking Poincaré sections, sect. 3.1.2. The intuitive idea is perhaps best visualized in the context of fluid flows. Suppose the flow exhibits an unstable coherent structure that – approximately– recurs often at different spatial dispositions. One can fit a 'template' to one recurrence of such structure, and describe other recurrences as its translations. A well chosen slice point belongs to such dynamically important equivalence class (i.e., group orbit). A slice is locally isomorphic to $\mathcal{M}/G$, in an open neighborhood of $\hat{x}'$. As is the case for the dynamical Poincaré sections, in general a single slice does not suffice to reduce $\mathcal{M} \to \mathcal{M}/G$ globally.

The Euclidian product of two vectors x, y is indicated in (10.42) by x-transpose times y, i.e., $x^T y = \sum_i^d x_i y_i$. More general bilinear norms $\langle x, y\rangle$ can be used, as long as they are G-invariant, i.e., constant on each irreducible subspace. An example is the quadratic Casimir (10.11).

Example 10.11 ***An SO(2) moving frame:*** *(continued from example 10.2) The SO(2) action*

$$(\hat{x}_1, \hat{x}_2) = (x_1 \cos\theta + x_2 \sin\theta,\ -x_1 \sin\theta + x_2 \cos\theta) \tag{10.45}$$

is regular on $\mathbb{R}^2\backslash\{0\}$. *Thus we can define a slice as a 'hyperplane' (here a mere line), through* $\hat{x}' = (0, 1)$, *with group tangent* $t' = (1, 0)$, *and ensure uniqueness by clockwise rotation into positive* x_2 *axis. Hence the reduced state space is the half-line* $x_1 = 0,\ \hat{x}_2 = x_2 > 0$. *The slice condition then simplifies to* $\hat{x}_1 = 0$ *and yields the explicit formula for the moving frame parameter*

$$\theta(x_1, x_2) = \tan^{-1}(x_1/x_2)\,, \tag{10.46}$$

i.e., the angle which rotates the point (x_1, x_2) *back to the slice, taking care that* $\tan^{-1}$ *distinguishes* (x_1, x_2) *plane quadrants correctly. Substituting (10.46) back to (10.45) and using* $\cos(\tan^{-1} a) = (1 + a^2)^{-1/2}$, $\sin(\tan^{-1} a) = a(1 + a^2)^{-1/2}$ *confirms* $\hat{x}_1 = 0$. *It also yields an explicit expression for the transformation to variables on the slice,*

$$\hat{x}_2 = \sqrt{x_1^2 + x_2^2}\,. \tag{10.47}$$

This was to be expected as $SO(2)$ *preserves lengths,* $x_1^2 + x_2^2 = \hat{x}_1^2 + \hat{x}_2^2$. *If dynamics is in plane and* $SO(2)$ *equivariant, the solutions can only be circles of radius* $(x_1^2 + x_2^2)^{1/2}$, *so this is the "rectification" of the harmonic oscillator by a change to polar coordinates, example 6.1. Still, it illustrates the sense in which the method of moving frames yields group invariants.* *(E. Siminos)*

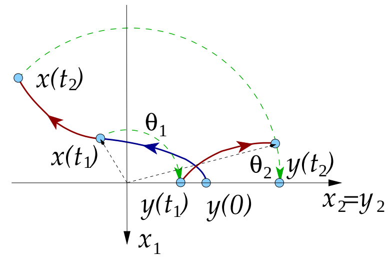

Figure 10.11: Method of moving frames for a flow SO(2)-equivariant under (10.18) with slice through $\hat{x}' = (0, 1, 0, 0, 0)$, group tangent $t' = (1, 0, 0, 0, 0)$. The clockwise orientation condition restricts the slice to half-hyperplane $\hat{x}_1 = 0$, $\hat{x}_2 > 0$. A trajectory started on the slice at $\hat{x}(0)$, evolves to a state space point with a non-zero $x_1(t_1)$. Compute the polar angle ϕ_1 of $x(t_1)$ in the (x_1, x_2) plane. Rotate $x(t_1)$ clockwise by ϕ_1 to $\hat{x}(t_1) = g(-\phi_1)\, x(t_1)$, so that the equivalent point on the circle lies on the slice, $\hat{x}_1(t_1) = 0$. Thus after every finite time step followed by a rotation the trajectory restarts from the $\hat{x}_1(t_k) = 0$ reduced state space.

The slice condition (10.42) fixes N directions; the remaining vectors $(\hat{x}_{N+1} \ldots \hat{x}_d)$ span the slice hyperplane. They are $d - N$ *fundamental invariants*, in the sense that any other invariant can be expressed in terms of them, and they are functionally independent. Thus they serve to distinguish orbits in the neighborhood of the slice-fixing point $\hat{x}'$, i.e., two points lie on the same group orbit if and only if all the fundamental invariants agree.

10.4.2 Dynamics within a slice

I made a wrong mistake.
—Yogi Berra

As an alternative to the post-processing approach of the preceding sections, we can proceed as follows: Split up the integration into a sequence of finite time steps, each followed by a rotation of the final point (and the whole coordinate frame with it; the 'moving frame') such that the next segment's initial point is in the *slice* fixed by a point $\hat{x}'$, see figure 10.11. It is tempting to see what happens if the steps are taken infinitesimal. As we shall see, we do get a flow restricted to the slice, but at a price.

Using decomposition (10.41) one can always write the full state space trajectory as $x(\tau) = g(\tau)\,\hat{x}(\tau)$, where the $(d-N)$-dimensional reduced state space trajectory $\hat{x}(\tau)$ is to be fixed by some condition, and $g(\tau)$ is then the corresponding curve on the N-dimensional group manifold of the group action that rotates $\hat{x}$ into x at time τ. The time derivative is then $\dot{x} = v(g\hat{x}) = \dot{g}\hat{x} + g\hat{v}$, with the reduced state space velocity field given by $\hat{v} = d\hat{x}/dt$. Rewriting this as $\hat{v} = g^{-1}v(g\,\hat{x}) - g^{-1}\dot{g}\,\hat{x}$ and using the equivariance condition (10.23) leads to

$$\hat{v} = v - g^{-1}\dot{g}\,\hat{x}\,.$$

The Lie group element (10.7) and its time derivative describe the group tangent flow

$$g^{-1}\dot{g} = g^{-1}\frac{d}{dt}e^{\phi\cdot\mathbf{T}} = \dot{\phi}\cdot\mathbf{T}\,.$$

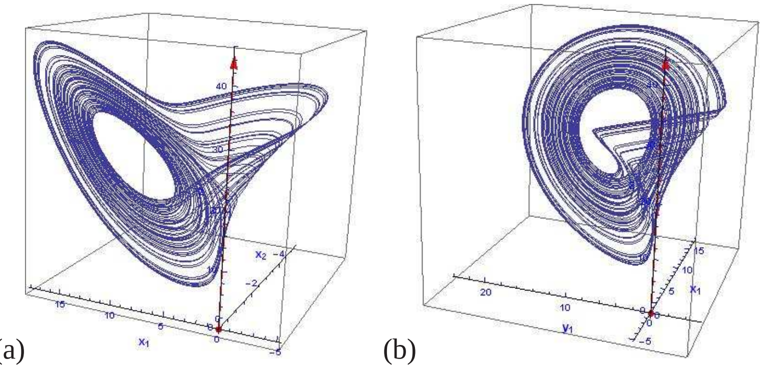

(a) (b)

Figure 10.12: A slice fixed by taking as a template a point on the complex Lorenz equations relative equilibrium group orbit, $\hat{x}' = x_{TW1}$. (a) The strange attractor of figure 10.1 in the reduced state space of (10.49), $\{x_1, x_2, z\}$ projection. (b) $\{x_2, y_2, z\}$ projection. The reduced state space complex Lorenz flow strange attractor of figure 10.1 now exhibits a discontinuity due to the vanishing denominator in (10.51).

This is the group tangent velocity $g^{-1}\dot{g}\,\hat{x} = \dot{\phi}\cdot t(\hat{x})$ evaluated at the point $\hat{x}$, i.e., with $g = 1$. The flow $\hat{v} = d\hat{x}/dt$ in the $(d-N)$ directions transverse to the group flow is now obtained by subtracting the flow along the group tangent direction,

$$\hat{v}(\hat{x}) = v(\hat{x}) - \dot{\phi}(\hat{x})\cdot t(\hat{x})\,, \tag{10.48}$$

for any factorization (10.41) of the flow of form $x(\tau) = g(\tau)\,\hat{x}(\tau)$. To integrate these equations we first have to fix a particular flow factorization by imposing conditions on $\hat{x}(\tau)$, and then integrate phases $\phi(\tau)$ on a given reduced state space trajectory $\hat{x}(\tau)$. exercise 10.31 exercise 10.32

Here we demand that the reduced state space is confined to a hyperplane slice. Substituting (10.48) into the time derivative of the fixed slice condition (10.43),

$$\hat{v}(\hat{x})^T t'_a = v(\hat{x})^T t'_a - \dot{\phi}_a\cdot t(\hat{x})^T t'_a = 0\,,$$

yields the equation for the group phases flow $\dot{\phi}$ for the slice fixed by $\hat{x}'$, together with the reduced state space $\hat{\mathcal{M}}$ flow $\hat{v}(\hat{x})$:

$$\begin{aligned} \hat{v}(\hat{x}) &= v(\hat{x}) - \dot{\phi}(\hat{x})\cdot t(\hat{x})\,, \qquad \hat{x}\in\hat{\mathcal{M}} && (10.49)\\ \dot{\phi}_a(\hat{x}) &= \frac{v(\hat{x})^T t'_a}{t(\hat{x})^T\cdot t'}\,. && (10.50)\end{aligned}$$

Each group orbit $\mathcal{M}_x = \{g\,x\,|\,g\in G\}$ is an equivalence class; method of slices represents the class by its single slice intersection point $\hat{x}$. By construction $\hat{v}^T t' = 0$, and the motion stays in the $(d-N)$-dimensional slice. We have thus replaced the original dynamical system $\{\mathcal{M}, f\}$ by a reduced system $\{\hat{\mathcal{M}}, \bar{f}\}$.

In the pattern recognition and 'template fitting' settings (10.50) is called the 'reconstruction equation.' Integrated together, the reduced state space trajectory (10.49) and $g(\tau) = \exp\{\phi(\tau)\cdot\mathbf{T}\}$, the integrated phase (10.50), reconstruct the full state space trajectory $x(\tau) = g(\tau)\,\hat{x}(\tau)$ from the reduced state space trajectory $\hat{x}(\tau)$, so no information about the flow is lost in the process of symmetry reduction. exercise 10.33 exercise 10.35

Example 10.12 ***A slice for complex Lorenz flow.*** *(continuation of example 10.6) Here we can use the fact that*

$$t(\hat{x})^T \cdot t' = \overline{x}^T \mathbf{T}^T \cdot \mathbf{T}\,\hat{x}' = \overline{x}_1 x_1' + \overline{x}_2 x_2' + \overline{y}_1 y_1' + \overline{y}_2 y_2'$$

is the dot-product restricted to the $m = 1$ 4-dimensional representation of $SO(2)$. A generic $\hat{x}'$ can be brought to form $\hat{x}' = (0, 1, y_1', y_2', z)$ by a rotation and rescaling. Then $\mathbf{T}\hat{x}' = (1, 0, y_2', -y_1', 0)$, and

$$\frac{v(\overline{x}) \cdot t'}{t(\overline{x}) \cdot t'} = -\frac{v_1 + v_3 y_2' - v_4 y_1'}{\overline{x}_2 + \overline{y}_1 y_1' + \overline{y}_2 y_2'} \,. \tag{10.51}$$

A long time trajectory of (10.49) with $\hat{x}'$ on the relative equilibrium TW_1 group orbit is shown in figure 10.12. As initial condition we chose the initial point (10.32) on the unstable manifold of TW_1, rotated back to the slice by angle ϕ as prescribed by (10.43). We show the part of the trajectory for $t \in [70, 100]$. The relative equilibrium TW_1, now an equilibrium of the reduced state space dynamics, organizes the flow into a Rössler type attractor (see figure 2.6). The denominator in (10.50) vanishes and the phase velocity $\dot{\phi}(\hat{x})$ diverges whenever the direction of group action on the reduced state space point is perpendicular to the direction of group action on the slice point $\hat{x}'$. While the reduced state space flow appears continuous in the $\{x_1, x_2, z\}$ projection, figure 10.12 (a), this singularity manifests itself as a discontinuity in the $\{x_2, y_2, z\}$ projection, figure 10.12 (b). The reduced state space complex Lorenz flow strange attractor of figure 10.1 now exhibits a discontinuity whenever the trajectory crosses this 3-dimensional subspace.

Slice flow equations (10.49) and (10.50) are pretty, but there is a trouble in the paradise. The slice flow encounters singularities in subsets of state space, with phase velocity $\dot{\phi}$ divergent whenever the denominator in (10.51) changes sign, see $\{x_2, y_2, z\}$ projection of figure 10.12 (b). Hence a single slice does not in general suffice to cover $\mathcal{M}/G$ globally.

10.5 Method of images: Hilbert bases

(E. Siminos and P. Cvitanović)

Erudite reader might wonder: why all this slicing and dicing, when the problem of symmetry reduction had been solved by Hilbert and Weyl nearly a century ago? Indeed, the most common approach to symmetry reduction is by means of a Hilbert invariant polynomial bases (9.27), motivated intuitively by existence of such nonlinear invariants as the rotationally-invariant length $r^2 = x_1^2 + x_2^2 + \cdots + x_d^2$, or, in Hamiltonian dynamics, the energy function. One trades in the equivariant state space coordinates $\{x_1, x_2, \cdots, x_d\}$ for a non-unique set of $m \geq d$ polynomials $\{u_1, u_2, \cdots, u_m\}$ invariant under the action of the symmetry group. These polynomials are linearly independent, but functionally dependent through $m - d + N$ relations called *syzygies*.

Example 10.13 ***An $SO(2)$ Hilbert basis.*** *(continued from example 9.18) The Hilbert basis*

$$u_1 = x_1^2 + x_2^2 \,, \qquad u_2 = y_1^2 + y_2^2 \,,$$

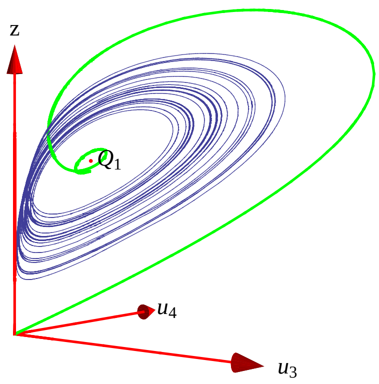

Figure 10.13: Invariant 'image' of complex Lorenz flow, figure 10.1, projected onto the invariant polynomials basis (10.52). Note the unstable manifold connection from the equilibrium EQ_0 at the origin to the strange attractor controlled by the rotation around relative equilibrium EQ_1 (the reduced state space image of TW_1); as in the Lorenz flow figure 3.4, natural measure close to EQ_0 is vanishingly small but non-zero.

$$\begin{aligned} u_3 &= x_1 y_2 - x_2 y_1 \,, \qquad u_4 = x_1 y_1 + x_2 y_2 \,, \\ u_5 &= z \,. \end{aligned} \tag{10.52}$$

is invariant under the $SO(2)$ action on a 5-dimensional state space (10.18). That implies, in particular, that the image of the full state space relative equilibrium TW_1 group orbit of figure 10.4 is the stationary equilibrium point EQ_1, see figure 10.13. The polynomials are linearly independent, but related through one syzygy,

$$u_1 u_2 - u_3^2 - u_4^2 = 0 \,, \tag{10.53}$$

yielding a 4-dimensional $\mathcal{M}/SO(2)$ reduced state space, a symmetry-invariant representation of the 5-dimensional $SO(2)$ equivariant dynamics. *(continued in example 10.14)*

The dynamical equations follow from the chain rule

$$\dot{u}_i = \frac{\partial u_i}{\partial x_j} \dot{x}_j \,, \tag{10.54}$$

upon substitution $\{x_1, x_2, \cdots, x_d\} \to \{u_1, u_2, \cdots, u_m\}$. One can either rewrite the dynamics in this basis or plot the 'image' of solutions computed in the original, equivariant basis in terms of these invariant polynomials. exercise 10.15

Example 10.14 ***Complex Lorenz equations in a Hilbert basis.*** *(continuation of example 10.13) Substitution of (10.2) and (10.52) into (10.54) yields complex Lorenz equations in terms of invariant polynomials:*

$$\begin{aligned} \dot{u}_1 &= 2\,\sigma\,(u_4 - u_1) \,, \\ \dot{u}_2 &= -2\,(u_2 - \rho_2\,u_3 - (\rho_1 - u_5)\,u_4) \,, \\ \dot{u}_3 &= -(\sigma + 1)\,u_3 + \rho_2\,u_1 + e\,u_4 \,, \\ \dot{u}_4 &= -(\sigma + 1)\,u_4 + (\rho_1 - u_5)\,u_1 + \sigma\,u_2 - e\,u_3 \,, \\ \dot{u}_5 &= u_4 - b\,u_5 \,. \end{aligned} \tag{10.55}$$

As far as visualization goes, we need neither construct nor integrate the invariant dynamics (10.55). It suffices to integrate the original, unreduced flow of Figure 10.1, but plot the solution in the image space, i.e., u_i invariant, Hilbert polynomial coordinates, as in figure 10.13. *(continued in example 10.15)*

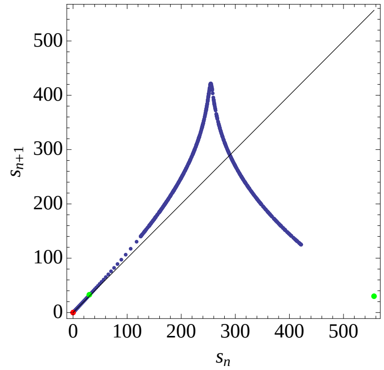

Figure 10.14: Return map to the Poincaré section $u_1 = u_4$ for complex Lorenz equations projected on invariant polynomials (10.52). The return map coordinate is the Euclidean arclength distance from TW_1, measured along the Poincaré section of its spiral-out unstable manifold, as for the Lorenz flow return map of example 11.4.

Reducing dimensionality of a dynamical system by elimination of variables through inclusion of syzygies such as (10.53) introduces singularities. Such elimination of variables, however, is not needed for visualization purposes; syzygies merely guarantee that the dynamics takes place on a submanifold in the projection on the $\{u_1, u_2, \cdots, u_m\}$ coordinates. However, when one *reconstructs* the dynamics in the original space $\mathcal{M}$ from its image $\mathcal{M}/G$, the transformations have singularities at the fixed-point subspaces of the isotropy subgroups in $\mathcal{M}$.

Example 10.15 ***Hilbert basis singularities.*** *(continuation of example 10.14) When one takes syzygies into account in rewriting a dynamical system, singularities are introduced. For instance, if we solve (10.53) for u_2 and substitute into (10.55), the reduced set of equations,*

$$\begin{aligned}
\dot{u}_1 &= 2\,\sigma\,(u_4 - u_1) \\
\dot{u}_3 &= -(\sigma + 1)\,u_3 + \rho_2\,u_1 + e\,u_4 \\
\dot{u}_4 &= -(\sigma + 1)\,u_4 + (\rho_1 - u_5)\,u_1 + \sigma\,(u_3^2 + u_4^2)/u_1 - e\,u_3 \\
\dot{u}_5 &= u_4 - b\,u_5\,,
\end{aligned} \tag{10.56}$$

is singular as $u_1 \to 0$. *(E. Siminos)*

Nevertheless we can now easily identify a suitable Poincaré section, guided by the Lorenz flow examples of chapter 9, as one that contains the z-axis and the image of the relative equilibrium TW_1, here defined by the condition $u_1 = u_4$. As in example 11.4, we construct the first return map using as coordinate the Euclidean arclength along the intersection of the unstable manifold of TW_1 with the Poincaré surface of section, see figure 10.14. Thus the goals set into the introduction to this chapter are attained: we have reduced the messy strange attractor of figure 10.1 to a 1-dimensional return map. As will be explained in example 11.4 for the Lorenz attractor, we now have the symbolic dynamics and can compute as many relative periodic orbits of the complex Lorenz flow as we wish, missing none.

What limits the utility of Hilbert basis methods are not such singularities, but rather the fact that the algebra needed to determine a Hilbert basis becomes computationally prohibitive as the dimension of the system or of the group increases. Moreover, even if such basis were available, rewriting the equations in an invariant polynomial basis seems impractical, so Hilbert basis computations appear not feasible beyond state space dimension of order ten. When our goal is to quotient continuous symmetries of high-dimensional flows, such as the Navier-Stokes flows, we need a more practical, workable framework. The method of moving frames of sect. 10.4 is one such minimalist alternative.

Résumé

The message: If a dynamical systems has a symmetry, use it! Here we have described how, and offered two approaches to continuous symmetry reduction. In the *method of slices* one fixes a 'slice' $(\hat{x} - \hat{x}')^T t' = 0$, a hyperplane normal to the group tangent t' that cuts across group orbits in the neighborhood of the slice-fixing point $\hat{x}'$. Each class of symmetry-equivalent points is represented by a single point, with the symmetry-reduced dynamics in the reduced state space $\mathcal{M}/G$ given by (10.49):

$$\hat{v} = v - \dot{\phi} \cdot t\,, \qquad \dot{\phi}_a = (v^T t'_a)/(t \cdot t')\,.$$

In practice one runs the dynamics in the full state space, and post-processes the trajectory by the method of moving frames. In the *Hilbert polynomial basis* approach one transforms the equivariant state space coordinates into invariant ones, by a nonlinear coordinate transformation

$$\{x_1, x_2, \cdots, x_d\} \to \{u_1, u_2, \cdots, u_m\} \quad + \quad \{syzygies\}\,,$$

and studies the invariant 'image' of dynamics (10.54) rewritten in terms of invariant coordinates.

In practice, continuous symmetry reduction is considerably more involved than the discrete symmetry reduction to a fundamental domain of chapter 9. Slices are only local sections of group orbits, and Hilbert polynomials are non-unique and difficult to compute for high-dimensional flows. However, there is no need to actually recast the dynamics in the new coordinates: either approach can be used as a visualization tool, with all computations carried out in the original coordinates, and then, when done, projecting the solutions onto the symmetry reduced state space by post-processing the data. The trick is to construct a good set of symmetry invariant Poincaré sections (see sect. 3.1), and that is always a dark art, with or without a symmetry.

We conclude with a few general observations: Higher dimensional dynamics requires study of compact invariant sets of higher dimension than 0-dimensional equilibria and 1-dimensional periodic orbits studied so far. In sect. 2.1.1 we made an attempt to classify 'all possible motions:' (1) equilibria, (2) periodic orbits, (3) everything else. Now one can discern in the fog of dynamics an outline of a more serious classification - long time dynamics takes place on the closure of a set of all invariant compact sets preserved by the dynamics, and those are: (1) 0-dimensional equilibria $\mathcal{M}_{EQ}$, (2) 1-dimensional periodic orbits $\mathcal{M}_p$, (3) global symmetry induced N-dimensional relative equilibria $\mathcal{M}_{TW}$, (4) (N+1)-dimensional relative periodic orbits $\mathcal{M}_p$, (5) terra incognita. We have some inklings of the 'terra incognita:' for example, in symplectic symmetry settings one finds KAM-tori, and in general dynamical settings we encounter *partially hyperbolic invariant M-tori*, isolated tori that are consequences of dynamics, not of a global symmetry. They are harder to compute than anything we have attempted so far, as they cannot be represented by a single relative periodic orbit, but require a numerical computation of full M-dimensional compact invariant sets and their infinite-dimensional linearized Jacobian matrices, marginal in M dimensions, and hyperbolic in the rest. We expect partially hyperbolic invariant tori to play important role in high-dimensional dynamics. In this chapter we have focused on the simplest example of such compact invariant sets, where invariant tori are a robust consequence of a global continuous symmetry of the dynamics. The direct product structure of a global symmetry that commutes with the flow enables us to reduce the dynamics to a desymmetrized $(d-1-N)$-dimensional reduced state space $\mathcal{M}/G$.

Relative equilibria and relative periodic orbits are the hallmark of systems with continuous symmetry. Amusingly, in this extension of 'periodic orbit' theory from unstable 1-dimensional closed periodic orbits to unstable (N+1)-dimensional compact manifolds $\mathcal{M}_p$ invariant under continuous symmetries, there are either no or proportionally few periodic orbits. In presence of a continuous symmetry, likelihood of finding a periodic orbit is *zero*. Relative periodic orbits are almost never eventually periodic, i.e., they almost never lie on periodic trajectories in the full state space, so looking for periodic orbits in systems with continuous symmetries is a fool's errand.

However, dynamical systems are often equivariant under a combination of continuous symmetries and discrete coordinate transformations of chapter 9, for example the orthogonal group O(n). In presence of discrete symmetries relative periodic orbits within discrete symmetry-invariant subspaces are eventually periodic. Atypical as they are (no generic chaotic orbit can ever enter these discrete invariant subspaces) they will be important for periodic orbit theory, as there the shortest orbits dominate, and they tend to be the most symmetric solutions. chapter 21

Commentary

Remark 10.1 A brief history of relativity, or, 'Desymmetrization and its discontents' (after Civilization and its discontents; continued from remark 9.1): The literature on symmetries in dynamical systems is immense, most of it deliriously unintelligible. Would it kill them to say 'symmetry of orbit p' instead of carrying on about 'isotropies, quotients, factors, normalizers, centralizers and stabilizers?' [10.9, 10.10, 10.8, 9.15] Group action being 'free, faithful, proper, regular?' Symmetry-reduced state space being 'orbitfold?' For the dynamical systems applications at hand we need only basic the Lie group facts, on the level of any standard group theory textbook [10.2]. We found Roger Penrose [10.3] introduction to the subject both enjoyable and understandable. Chapter 2. of ref. [10.4] offers a pedagogical introduction to Lie groups of transformations, and Nakahara [10.5] to Lie derivatives and brackets. The presentation given here is in part based on Siminos thesis [10.6] and ref. [10.7]. The reader is referred to the monographs of Golubitsky and Stewart [10.8], Hoyle [10.9], Olver [10.11], Bredon [10.12], and Krupa [10.13] for more depth and rigor than would be wise to wade into here.

Relative equilibria and relative periodic solutions are related by symmetry reduction to equilibria and periodic solutions of the reduced dynamics. They appear in many physical applications, such as celestial mechanics, molecular dynamics, motion of rigid bodies, nonlinear waves, spiralling patterns, and fluid mechanics. A relative equilibrium is a solution which travels along an orbit of the symmetry group at constant speed; an introduction to them is given, for example, in Marsden [**?**]. According to Cushman, Bates [10.14] and Yoder [10.15], C. Huygens [10.16] understood the relative equilibria of a spherical pendulum many years before publishing them in 1673. A reduction of the translation symmetry was obtained by Jacobi (for a modern, symplectic implementation, see Laskar *et al.* [10.17]). In 1892 German sociologist Vierkandt [10.18] showed that on a symmetry-reduced space (the constrained velocity phase space modulo the action of the group of Euclidean motions of the plane) all orbits of the rolling disk system are periodic [10.19]. According to Chenciner [10.20], the first attempt to find (relative) periodic solutions of the N-body problem was the 1896 short note by Poincaré [10.21], in the context of the 3-body problem. Poincaré named such solutions 'relative.' Relative equilibria of the N-body problem (known in this context as the Lagrange points, stationary in the co-rotating frame) are circular motions in the inertial frame, and relative periodic orbits correspond to quasiperiodic motions in the inertial frame. For relative periodic orbits in celestial mechanics see also ref. [10.22]. A striking application of relative periodic orbits has been the discovery of "choreographies" in the N-body problems [10.23, 10.24, 10.25].

The modern story on equivariance and dynamical systems starts perhaps with S. Smale [10.26] and M. Field [10.27], and on bifurcations in presence of symmetries with Ruelle [10.28]. Ruelle proves that the stability matrix/Jacobian matrix evaluated at an equilibrium/fixed point $x \in \mathcal{M}_G$ decomposes into linear irreducible representations of G, and that stable/unstable manifold continuations of its eigenvectors inherit their symmetry properties, and shows that an equilibrium can bifurcate to a rotationally invariant periodic orbit (i.e., relative equilibrium).

Gilmore and Lettelier monograph [10.29] offers a very clear, detailed and user friendly discussion of symmetry reduction by means of Hilbert polynomial bases (do not look for 'Hilbert' in the index, though). Vladimirov, Toronov and Derbov [10.30] use an invariant polynomial basis different from (10.52) to study bounding manifolds of the symmetry reduced complex Lorenz flow and its homoclinic bifurcations. There is no general strategy how to construct a Hilbert basis; clever low-dimensional examples have been constructed case-by-case. The example 10.13, with one obvious syzygy, is also misleading - syzygies proliferate rapidly with increase in dimensionality. The determination of a Hilbert basis appears computationally prohibitive for state space dimensions larger than ten [10.31, 10.32], and rewriting the equations of motions in invariant polynomial bases appears impractical for high-dimensional flows. Thus, by 1920's the problem of rewriting equivariant flows as invariant ones was solved by Hilbert and Weyl, but at the cost of introducing largely arbitrary extra dimensions, with the reduced flows on manifolds of lowered dimensions, constrained by sets of syzygies. Cartan found this unsatisfactory, and in 1935 he introduced [10.33] the notion of a *moving frame*, a map from a manifold to a Lie group, which seeks no invariant polynomial basis, but instead rewrites the reduced $\mathcal{M}/G$ flow in terms of $d - N$ *fundamental invariants* defined by a generalization of the Poincaré section, a slice that cuts across all group orbits in some open neighborhood. Fels and Olver view the method as an alternative to the Gröbner bases methods for computing Hilbert polynomials, to compute functionally independent fundamental invariant bases for general group actions (with no explicit connection to dynamics, differential equations or symmetry reduction). 'Fundamental' here means that they can be used to generate all other invariants. Olver's monograph [10.11] is pedagogical, but does not describe the original Cartan's method. Fels and Olver papers [10.34, 10.35] are lengthy and technical. They refer to Cartan's method as method of 'moving frames' and view it as a special and less rigorous case of their 'moving coframe' method. The name 'moving coframes' arises through the use of Maurer-Cartan form which is a coframe on the Lie group G, i.e., they form a pointwise basis for the cotangent space. In refs. [10.6, 10.7] the invariant bases generated by the moving frame method are used as a basis to project a full state space trajectory to the slice (i.e., the $\mathcal{M}/G$ reduced state space).

The basic idea of the 'method of slices' is intuitive and frequently reinvented, often under a different name; for example, it is stated without attribution as the problem 1. of Sect. 6.2 of Arnol'd *Ordinary Differential Equations* [10.36]. The factorization (10.41) is stated on p. 31 of Anosov and Arnol'd [10.37], who note, without further elaboration, that in the vicinity of a point which is not fixed by the group one can reduce the order of a system of differential equations by the dimension of the group. Ref. [10.38] refers to symmetry reduction as 'lowering the order.' For the definition of 'slice' see, for example, Chossat and Lauterbach [10.32]. Briefly, a submanifold $\mathcal{M}_{\hat{x}'}$ containing $\hat{x}'$ is called a *slice* through $\hat{x}'$ if it is invariant under isotropy $G_{\hat{x}'(\mathcal{M}_{\hat{x}'})} = \mathcal{M}_{\hat{x}'}$. If $\hat{x}'$ is a fixed point of G, than slice is invariant under the whole group. The slice theorem is explained, for example, in Encyclopaedia of Mathematics. Slices tend to be discussed in contexts much more difficult than our application - symplectic groups, sections in absence of global charts, non-compact Lie groups. We follow refs. [10.39] in referring to a local group-orbit section as a 'slice.' Refs. [10.12, 10.40] and others refer to global group-orbit sections as 'cross-sections,' a term that we would rather avoid, as it already has a different and well established meaning in physics. Duistermaat and Kolk [10.41] refer to 'slices,' but the usage goes back at least to Guillemin and Sternberg [10.40] in 1984, Palais [10.42] in 1961 and Mastow [10.43] in 1957. Bredon [10.12] discusses both cross-sections and slices. Guillemin and Sternberg [10.40] define the 'cross-section,' but emphasize that finding it is very rare: "existence of a global section is a very stringent condition on a group action. The notion of 'slice' is weaker but has a much broader range of existence."

Several important fluid dynamics flows exhibit continuous symmetries which are either SO(2) or products of SO(2) groups, each of which act on different coordinates of the state space. The Kuramoto-Sivashinsky equations [26.3, 26.4], plane Couette flow [H.31, 26.15, 10.55, B.1], and pipe flow [10.56, 10.57] all have continuous symmetries of this form. In the 1982 paper Rand [10.58] explains how presence of continuous symmetries gives rise to rotating and modulated rotating (quasiperiodic) waves in fluid dynamics. Haller and Mezić [10.59] reduce symmetries of three-dimensional volume-preserving flows and reinvent method of moving frames, under the name 'orbit projection map.' There is extensive literature on reduction of symplectic manifolds with symmetry; Marsden and Weinstein 1974 article [10.60] is an important early reference. Then there are studies of the reduced phase spaces for vortices moving on a sphere such as ref. [10.61], and many, many others.

Reaction-diffusion systems are often equivariant with respect to the action of a finite dimensional (not necessarily compact) Lie group. Spiral wave formation in such nonlinear excitable media was first observed in 1970 by Zaikin and Zhabotinsky [10.44]. Winfree [10.45, 10.46] noted that spiral tips execute meandering motions. Barkley and collaborators [10.47, 10.48] showed that the noncompact Euclidean symmetry of this class of systems precludes nonlinear entrainment of translational and rotational drifts and that the interaction of the Hopf and the Euclidean eigenmodes leads to observed quasiperiodic and meandering behaviors. Fiedler, in the influential 1995 talk at the Newton Institute, and Fiedler, Sandstede, Wulff, Turaev and Scheel [10.49, 10.50, 10.51, 10.52] treat Euclidean symmetry bifurcations in the context of spiral wave formation. The central idea is to utilize the semidirect product structure of the Euclidean group $E(2)$ to transform the flow into a 'skew product' form, with a part orthogonal to the group orbit, and the other part within it, as in (10.49). They refer to a linear slice $\hat{\mathcal{M}}$ near relative equilibrium as a *Palais slice*, with Palais coordinates. As the choice of the slice is arbitrary, these coordinates are not unique. According to these authors, the skew product flow was first written down by Mielke [10.53], in the context of buckling in the elasticity theory. However, this decomposition is no doubt much older. For example, it was used by Krupa [10.13, 10.32] in his local slice study of bifurcations of relative equilibria. Biktashev, Holden, and Nikolaev [10.54] cite Anosov and Arnol'd [10.37] for the 'well-known' factorization (10.41) and write down the slice flow equations (10.49).

Neither Fiedler *et al.* [10.49] nor Biktashev *et al.* [10.54] implemented their methods numerically. That was done by Rowley and Marsden for the Kuramoto-Sivashinsky [10.39] and the Burgers [10.62] equations, and Beyn and Thümmler [10.63, 10.64] for a number of reaction-diffusion systems, described by parabolic partial differential equations on unbounded domains. We recommend the Barkley paper [10.48] for a clear explanation of how the Euclidean symmetry leads to spirals, and the Beyn and Thümmler paper [10.63] for inspirational concrete examples of how 'freezing'/'slicing' simplifies the dynamics of rotational, traveling and spiraling relative equilibria. Beyn and Thümmler write the solution as a composition of the action of a time dependent group element $g(t)$ with a 'frozen,' in-slice solution $\hat{u}(t)$ (10.41). In their nomenclature, making a relative equilibrium stationary by going to a co-moving frame is 'freezing' the traveling wave, and the imposition of the phase condition (i.e., slice condition (10.42)) is the 'freezing ansatz.' They find it more convenient to make use of the equivariance by extending the state space rather than reducing it, by adding an additional parameter and a phase condition. The 'freezing ansatz' [10.63] is identical to the Rowley and Marsden [10.62] and our slicing, except that 'freezing' is formulated as an additional constraint, just as when we compute periodic orbits of ODEs we add Poincaré section as an additional constraint, i.e., increase the dimensionality of the problem by 1 for every continuous symmetry (see sect. 13.4). section 13.4

Derivation of sect. 10.4.2 follows most closely Rowley and Marsden [10.62] who, in the pattern recognition setting refer to the slice point as a 'template,' and call (10.50) the 'reconstruction equation' [**?**, 10.65]. They also describe the 'method of connections' (called 'orthogonality of time and group orbit at successive times' in ref. [10.63]), for which the reconstruction equation (10.50) denominator is $t(\hat{x})^T \cdot t(\hat{x})$ and thus nonvanishing as long as the action of the group is regular. This avoids the spurious slice singularities, but it is not clear what the 'method of connections' buys us otherwise. It does not reduce the dimensionality of the state space, and it accrues 'geometric phases' which prevent relative periodic orbits from closing into periodic orbits. Geometric phase in laser equations, including complex Lorenz equations, has been studied in ref. [10.66, 10.67, 10.69, 10.70, 10.71]. Another theorist's temptation is to hope that a continuous symmetry would lead us to a conserved quantity. However, Noether theorem requires that equations of motion be cast in Lagrangian form and that the Lagrangian exhibits variational symmetries [10.72, 10.73]. Such variational symmetries are hard to find for dissipative systems.

Sect. 10.1.2 title 'Lie groups for cyclists' is bit of a joke in more ways than one. First, 'cyclist,' 'pedestrian' throughout ChaosBook.org refer jokingly both to the title of Lipkin's *Lie groups for pedestrians* [10.74] and to our preoccupations with actual cycling. Lipkin's 'pedestrian' is fluent in Quantum Field Theory, but wobbly on Dynkin diagrams. More to the point, it is impossible to dispose of Lie groups in a page of text. As a counterdote to the 1-page summary of sect. 10.1.2, consider reading Gilmore's monograph [10.75] which offers a quirky, personal and enjoyable distillation of a lifetime of pondering Lie groups. As seems to be the case with any textbook on Lie groups, it will not help you with the problem at hand, but it is the only place you can learn both what

Galois actually did when he invented the theory of finite groups in 1830, and what, inspired by Galois, Lie actually did in his 1874 study of symmetries of ODEs. Gilmore also explains many things that we pass over in silence here, such as matrix groups, group manifolds, and compact groups.

One would think that with all this literature the case is shut and closed, but not so. Applied mathematicians are inordinately fond of bifurcations, and almost all of the previous work focuses on equilibria, relative equilibria, and their bifurcations, and for these problems a single slice works well. Only when one tries to describe the totality of chaotic orbits does the non-global nature of slices become a serious nuisance.

(E. Siminos and P. Cvitanović)

Remark 10.2 Complex Lorenz equations (10.1) were introduced by Gibbon and McGuinness [10.76, 10.77] as a low-dimensional model of baroclinic instability in the atmosphere. They are a generalization of Lorenz equations (2.12). Ning and Haken [10.78] have shown that equations isomorphic to complex Lorenz equations also appear as a truncation of Maxwell-Bloch equations describing a single mode, detuned, ring laser. They set $e + \rho_2 = 0$ so that SO(2)-orbits of detuned equilibria exist [10.77]. Zeghlache and Mandel [**?**] also use equations isomorphic to complex Lorenz equations with $e+\rho_2 = 0$ in their studies of detuned ring lasers. This choice is 'degenerate' in the sense that it leads to non-generic bifurcations. As existence of relative equilibria in systems with SO(2) symmetry is the generic situation, we follow Bakasov and Abraham [10.79] who set $\rho_2 = 0$ and $e \neq 0$ in order to describe detuned lasers. Here, however, we are not interested in the physical applications of these equations; rather, we study them as a simple example of a dynamical system with continuous (but no discrete) symmetries, with a view of testing methods of reducing the dynamics to a lower-dimensional reduced state space. Complex Lorenz flow examples and exercises in this chapter are based on E. Siminos thesis [10.6] and R. Wilczak project report [10.80].

Remark 10.3 Velocity *vs.* Speed *Velocity* is a vector, the rate at which the object changes its position. *Speed*, or the magnitude of the velocity, is a scalar quantity which describes how fast an object moves. We denote the rate of change of group phases, or the *phase velocity* by the vector $c = (\dot{\phi}_1, \cdots, \dot{\phi}_N) = (c_1, \cdots, c_N)$, a component for each of the N continuous symmetry parameters. These are converted to state space velocity components along the group tangents by

$$v(x) = c(t) \cdot t(x) . \tag{10.57}$$

For rotational waves these are called "angular velocities."

Remark 10.4 Killing fields. The symmetry tangent vector fields discussed here are a special case of Killing vector fields of Riemannian geometry and special relativity. If this poetry warms the cockles of your heart, hang on. From wikipedia (this wikipedia might also be useful): A Killing vector field is a set of infinitesimal generators of isometries on a Riemannian manifold that preserve the metric. Flows generated by Killing fields are continuous isometries of the manifold. The flow generates a symmetry, in the sense that moving each point on an object the same distance in the direction of the Killing vector field will not distort distances on the object. A vector field X is a Killing field if the Lie derivative with respect to X of the metric g vanishes:

$$\mathcal{L}_X g = 0 . \tag{10.58}$$

Killing vector fields can also be defined on any (possibly nonmetric) manifold $\mathcal{M}$ if we take any Lie group G acting on it instead of the group of isometries. In this broader sense, a Killing vector field is the pushforward of a left invariant vector field on G by the group action. The space of the Killing vector fields is isomorphic to the Lie algebra $\mathfrak{g}$ of G.

If the equations of motion can be cast in Lagrangian form, with the Lagrangian exhibiting variational symmetries [10.72, 10.73], Noether theorem associates a conserved quantity with each Killing vector.

(E. Siminos and P. Cvitanović)

Exercises

10.1. **Visualizations of the 5-dimensional complex Lorenz flow:** Plot complex Lorenz flow projected on any three of the five $\{x_1, x_2, y_1, y_2, z\}$ axes. Experiment with different visualizations.

10.2. **SO(2) rotations in a plane:** Show by exponentiation (10.7) that the SO(2) Lie algebra element $\mathbf{T}$ generates rotation g in a plane,

$$\begin{aligned} g(\theta) &= e^{\mathbf{T}\theta} = \cos\theta \begin{pmatrix} 1 & 0 \\ 0 & 1 \end{pmatrix} + \sin\theta \begin{pmatrix} 0 & 1 \\ -1 & 0 \end{pmatrix} \\ &= \begin{pmatrix} \cos\theta & \sin\theta \\ -\sin\theta & \cos\theta \end{pmatrix}. \end{aligned} \tag{10.59}$$

10.3. **Invariance under fractional rotations.** Argue that if the isotropy group of the velocity field $v(x)$ is the discrete subgroup C_m of SO(2) rotations about an axis (let's say the 'z-axis'),

$$C^{1/m}v(x) = v(C^{1/m}x) = v(x)\,, \qquad (C^{1/m})^m = e\,,$$

the only non-zero components of Fourier-transformed equations of motion are a_{jm} for $j = 1, 2, \cdots$. Argue that the Fourier representation is then the quotient map of the dynamics, $\mathcal{M}/C_m$. (Hint: this sounds much fancier than what is - think first of how it applies to the Lorenz system and the 3-disk pinball.)

10.4. **U(1) equivariance of complex Lorenz equations for finite angles:** Show that the vector field in complex Lorenz equations (10.1) is equivariant under (10.7), the unitary group U(1) acting on $\mathbb{R}^5 \cong \mathbb{C}^2 \times \mathbb{R}$ by

$$g(\theta)(x, y, z) = (e^{i\theta}x, e^{i\theta}y, z)\,, \quad \theta \in [0, 2\pi)\,. \tag{10.60}$$

(E. Siminos)

10.5. **SO(2) equivariance of complex Lorenz equations for finite angles:** Show that complex Lorenz equations (10.2) are equivariant under rotation for finite angles.

10.6. **Stability matrix of complex Lorenz flow:** Compute the stability matrix (10.26) for complex Lorenz equations (10.2).

10.7. **SO(2) equivariance of complex Lorenz equations for infinitesimal angles.** Show that complex Lorenz equations are equivariant under infinitesimal SO(2) rotations.

10.8. **A 2-mode SO(2)-equivariant flow:** Complex Lorenz equations (10.1) of Gibbon and McGuinness [10.76] have a degenerate 4-dimensional subspace, with SO(2) acting only in its lowest non-trivial representation. Here is a possible model, still 5-dimensional, but with SO(2) acting in the two lowest representations. Such models arise as truncations of Fourier-basis representations of PDEs on periodic domains. In the complex form, the simplest such modification of complex Lorenz equations may be the "2-mode" system

$$\begin{aligned} \dot{x} &= -\sigma x + \sigma x^* y \\ \dot{y} &= (\rho - z)x^2 - ay \\ \dot{z} &= -bz + \frac{1}{2}\left(x^2 y^* + x^{*2} y\right)\,, \end{aligned} \tag{10.61}$$

where x, y, ρ, a are complex and z, b, σ are real. Rewritten in terms of real variables $x = x_1 + i\,x_2$, $y = y_1 + i\,y_2$ this is a 5-dimensional first order ODE system

$$\begin{aligned} \dot{x}_1 &= -\sigma x_1 + \sigma(x_1 y_1 - x_2 y_2) \\ \dot{x}_2 &= -\sigma x_2 + \sigma(x_1 y_2 - x_2 y_1) \end{aligned}$$

$$
\begin{aligned}
\dot{y}_1 &= -y_1 + e y_2 + (\rho_1 - z)(x_1^2 - x_2^2) - 2\rho_2 x_1 x_2 \\
\dot{y}_2 &= -y_2 - e y_1 + \rho_2 (x_1^2 - x_2^2) + (\rho_1 - z)(2 x_1 x_2) \\
\dot{z} &= -bz + (x_1^2 - x_2^2) y_1 + 2 x_1 x_2 y_2 \,.
\end{aligned}
\qquad (10.62)
$$

Verify (10.62) by substituting $x = x_1 + i\, x_2$, $y = y_1 + i\, y_2$, $\rho = \rho_1 + i\, \rho_2$, $a = 1 + i\, e$ into the complex 2-mode equations (10.61).

10.9. **U(1) equivariance of 2-mode system for finite angles:** Show that 2-mode system (10.61) is equivariant under rotation for finite angles.

10.10. **SO(2) equivariance of the 2-mode system for infinitesimal angles.** Verify that the 2-mode system (10.62) is equivariant under infinitesimal SO(2) rotations (10.18) by showing that the stability matrix (4.3) for the system is given by $A =$

$$
\begin{pmatrix}
\sigma(y_1 - 1) & \sigma y_2 & \sigma x_1 & \sigma x_2 & 0 \\
\sigma y_2 & -\sigma(y_1 + 1) & -\sigma x_2 & \sigma x_1 & 0 \\
2\rho_1 x_1 - 2\rho_2 x_2 - 2 x_1 z & 2 x_2 z - 2\rho_2 x_1 - 2\rho_1 x_2 & -1 & e & x_2^2 - x_1^2 \\
2\rho_1 x_2 + 2\rho_2 x_1 - 2 x_2 z & 2\rho_1 x_1 - 2\rho_2 x_2 - 2 x_1 z & -e & -1 & -2 x_1 x_2 \\
2 x_1 y_1 + 2 x_2 y_2 & 2 x_1 y_2 - 2 x_2 y_1 & x_1^2 - x_2^2 & 2 x_1 x_2 & -b
\end{pmatrix}
\qquad (10.63)
$$

and substituting the Lie algebra generator

$$
\mathbf{T} = \begin{pmatrix}
0 & 1 & 0 & 0 & 0 \\
-1 & 0 & 0 & 0 & 0 \\
0 & 0 & 0 & 2 & 0 \\
0 & 0 & -2 & 0 & 0 \\
0 & 0 & 0 & 0 & 0
\end{pmatrix}
\qquad (10.64)
$$

and the stability matrix (10.63) into the equivariance condition (10.24).

10.11. **Visualizations of the 5-dimensional 2-mode system:** Plot 2-mode system projected on any three of the five $\{x_1, x_2, y_1, y_2, z\}$ axes. For complex Lorenz flow numerical examples we have set the parameters to $\rho_1 = 28$, $\rho_2 = 0$, $b = 8/3$, $\sigma = 10$, $e = 1/10$, but here you will have to play with them until you find something that looks interestingly chaotic. Experiment with different visualizations. It's a big mess - have no clue what parameters to take, what the trajectory will do.

10.12. **Discover the equivariance of a given flow:** Suppose you were given complex Lorenz equations, but nobody told you they are SO(2) equivariant. More generally, you might encounter a flow without realizing that it has a continuous symmetry - how would you discover it?

10.13. **Equilibria of complex Lorenz equations:** Find all equilibria of complex Lorenz equations. Hint: Equilibria come either in the fixed Fix (G) subspace, or on a group orbit.

10.14. **More equilibria of complex Lorenz equations:** In exercise 10.13 we found only one equilibrium of complex Lorenz equations. The Ning and Haken [10.78] version of complex Lorenz equations (a truncation of Maxwell-Bloch equations describing a single mode ring laser) sets $e + \rho_2 = 0$ so that a detuned equilibrium exists. Test your routines on 2 cases: (a) $e = 0$, $\rho_2 = 0$. As discussed by Siminos [10.6], reality of parameters a, ρ in (10.1) implies existence of a discrete C_2 symmetry. (b) $e + \rho_2 = 0$, $e \neq 0$. You might want to compare results with those of Ning and Haken.

10.15. **Complex Lorenz equations in a Hilbert basis.** (continuation of example 10.13) Derive complex Lorenz equations (10.55) in terms of invariant polynomials (10.55), plot the strange attractor in projections you find illuminating (one example is figure 10.13).

10.16. **Hilbert basis singularities.** When one takes syzygies into account in rewriting a dynamical system, singularities are introduced. For instance, eliminate u_2 using the syzygy, and show that you get the reduced set of equations,

$$
\begin{aligned}
\dot{u}_1 &= 2\,\sigma\,(u_4 - u_1) \\
\dot{u}_3 &= -(\sigma + 1)\, u_3 + \rho_2\, u_1 + e\, u_4 \\
\dot{u}_4 &= -(\sigma + 1)\, u_4 + (\rho_1 - u_5)\, u_1 + \sigma\,(u_3^2 + u_4^2)/u_1 - \\
\dot{u}_5 &= u_4 - b\, u_5 \,,
\end{aligned}
\qquad (10
$$

singular as $u_1 \to 0$. (E. Siminos)

10.17. **Complex Lorenz equations in polar coordinates.** Rewrite complex Lorenz equations from Cartesian to polar coordinates, using $(x_1, x_2, y_1, y_2, z) =$

$$
(r_1 \cos\theta_1, r_1 \sin\theta_1, r_2 \cos\theta_2, r_2 \sin\theta_2, z)\,, \qquad (10.66)
$$

where $r_1 \geq 0\,, r_2 \geq 0$. Show that in polar coordinates the equations take form

$$
\begin{pmatrix} \dot{r}_1 \\ \dot{\theta}_1 \\ \dot{r}_2 \\ \dot{\theta}_2 \\ \dot{z} \end{pmatrix}
=
\begin{pmatrix}
-\sigma\,(r_1 - r_2 \cos\theta) \\
-\sigma \frac{r_2}{r_1} \sin\theta \\
-r_2 + r_1\,((\rho_1 - z)\cos\theta - \rho_2 \sin\theta) \\
e + \frac{r_1}{r_2}\,((\rho_1 - z)\sin\theta + \rho_2 \cos\theta) \\
-bz + r_1 r_2 \cos\theta
\end{pmatrix},
$$

where angles always appear in the combination $\theta = \theta_1 - \theta_2$ We know from classical mechanics that for translationally or rotationally invariant flows the relative distance is invariant (that is why one speaks of 'relative' equilibria), hence we introduce a variable $\theta = \theta_1 - \theta_2$. Show that this new variable allows us to rewrite the complex Lorenz equations as 4 coupled polar coordinates equations:

$$
\begin{pmatrix} \dot{r}_1 \\ \dot{r}_2 \\ \dot{\theta} \\ \dot{z} \end{pmatrix}
=
\begin{pmatrix}
-\sigma\,(r_1 - r_2 \cos\theta) \\
-r_2 + (\rho_1 - z) r_1 \cos\theta \\
-e - \left(\sigma \frac{r_2}{r_1} + (\rho_1 - z)\frac{r_1}{r_2}\right) \sin\theta \\
-bz + r_1 r_2 \cos\theta
\end{pmatrix}
(10.67)
$$

where we have set $\rho_2 = 0$. (hints: review (6.4), example 6.1, exercise 6.1, and (10.54))

10.18. **2-mode system in polar coordinates.** Show that the 2-mode system (10.62) rewritten in polar coordinates (10.66) is given by

$$\begin{aligned}
\dot{r}_1 &= -\sigma r_1 + \sigma r_1 r_2 \cos(\theta) \\
\dot{r}_2 &= -r_2 + r_1^2((\rho_1 - z)\cos(\theta) - \rho_2 \sin(\theta)) \\
\dot{\theta}_1 &= -\sigma r_2 \sin(\theta)\,, \quad \dot{\theta}_2 = -e + \frac{r_1^2}{r_2}((\rho_1 - z)\sin(\theta) + \rho_2\cos(\theta)) \\
\dot{z} &= -bz + \frac{r_1^2}{r_2}\cos(\theta)\,,
\end{aligned} \qquad (10.68)$$

where $\theta = 2\theta_1 - \theta_2$. Rewriting the angular part as $\dot{\theta} = 2\dot{\theta}_1 - \dot{\theta}_2$, we have

$$\dot{\theta} = e - \frac{r_1^2}{r_2}((\rho_1 - z)\sin(\theta) + \rho_2\cos(\theta)) - 2r_2\sigma\sin(\theta)\,. \qquad (10.69)$$

D. Borrero

10.19. **Visualizations of the complex Lorenz flow in polar coordinates:**

Plot a long-time solution of (10.67) and show that the polar representation introduces singularities into what initially was a smooth flow:

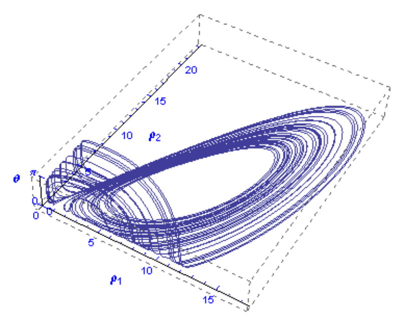

We shall encounter the same problem in implementing the $x_1 = 0$ slice, . θ is very small until the trajectory approaches either $r_1 \to 0$ or $r_2 \to 0$, where `Mathematica` continues through the singularity by a rapid change of θ by π. The fixed Fix (G) subspace $(r_1, r_2, \theta, z) = (0, 0, \theta, z)$ separates the two folds of the attractor.

Plot complex Lorenz flow projected on any three of the $\{r_1, r_2, \theta, z\}$ coordinates. Experiment with different visualizations. The flow is singular as $r_j \to 0$, with angle θ_j going through a rapid change there: is that a problem? Does it make sense to insist on $r_1 \geq 0\,, r_2 \geq 0$, or should one let them have either sign in order that the θ trajectory be continuous?

10.20. **Computing the relative equilibrium TW_1:** The two rotation angles θ_1 and θ_2 change in time, but at the relative equilibria the difference between them is constant, $\dot{\theta} = 0$. Find the relative equilibria of the complex Lorenz equations by finding the equilibria of the system in polar coordinates (10.67). Show that

(a) The relative equilibrium (hereafter referred to [10.6] as TW_1) is given by

$$\begin{aligned}
(r_1, r_2, \theta, z) \;=\; &\Big(\sqrt{b\,(\rho_1 - d)},\ \sqrt{bd\,(\rho_1 - d)}, \\
&\cos^{-1}\big(1/\sqrt{d}\big), \rho_1 - d\Big)\,,
\end{aligned} \qquad (10.70)$$

where $d = 1 + e^2/(\sigma + 1)^2$,

(b) The angular velocity of relative equilibrium TW_1 is

$$\dot{\theta}_i = \sigma e/(\sigma + 1)\,, \qquad (10.71)$$

with the period $T_{TW_1} = 2\pi(\sigma + 1)/\sigma e$.

10.21. **Relative equilibrium TW_1 in polar coordinates:** Plot the equilibrium TW_1 in polar coordinates.

10.22. **Relative equilibrium TW_1 in Cartesian coordinates:** Show that for (10.2) parameter values,

$$\begin{aligned}
x_{TW_1} &= (x_1, x_2, y_1, y_2, z) \\
&= (8.4849, 0.077135, 8.4856, 0, 26.999)\,,
\end{aligned} \qquad (10.72)$$

is a point on the TW_1 orbit. Plot the relative equilibrium TW_1 in Cartesian coordinates. State the velocity of relative equilibrium, compare with the imaginary part of the complex stability eigenvalue, and explain the two time scales visible in the 'horn', as well as the expansion rate per turn of the spiral.

10.23. **The relative equilibria of the 2-mode system:** Find the relative equilibria of the 2-mode system by finding the equilibria of the system in polar coordinates (10.67).

10.24. **Plotting the relative equilibria of the 2-mode system in polar coordinates:** Plot the relative equilibria of the 2-mode system in polar coordinates.

10.25. **Plotting the relative equilibria of the 2-mode system in Cartesian coordinates:** Plot the relative equilibria of the 2-mode system in Cartesian coordinates.

10.26. **Eigenvalues and eigenvectors of TW_1 stability matrix:** Compute the eigenvalues and eigenvectors of the stability matrix (10.26) evaluated at TW_1 and using the (10.2) parameter values, in (a) Cartesian coordinates, (b) polar coordinates.

10.27. **The eigen-system of TW_1 stability matrix in polar coordinates:** Plot the eigenvectors of A at TW_1 in polar coordinates, as well as the complex Lorenz flow at values very near TW_1.

10.28. **Eigenvalues and eigenvectors of EQ_0 stability matrix:** Find the eigenvalues and the eigenvectors of the stability matrix A (10.26) at $EQ_0 = (0, 0, 0, 0, 0)$ determined in exercise 10.13. ChaosBook convention is to order eigenvalues from most positive (unstable) to the most negative. Follow that. Replace complex eigenvectors by the real, imaginary parts, so you can plot them in (real) state space.

10.29. **The eigen-system of the stability matrix at EQ_0:** Plot the eigenvectors of A at EQ_0 and the complex Lorenz flow at values very close to EQ_0.

10.30. **SO(2) or harmonic oscillator slice:** Construct a moving frame slice for action of SO(2) on $\mathbb{R}^2$

$$(x, y) \mapsto (x \cos\theta - y \sin\theta,\ x \sin\theta + y \cos\theta)$$

by, for instance, the positive y axis: $x = 0$, $y > 0$. Write out explicitly the group transformations that bring any point back to the slice. What invariant is preserved by this construction? (E. Siminos)

10.31. **State space reduction by a slice, ODE formulation:** Replace integration of the complex Lorenz equations by a sequence of finite time steps, each followed by a rotation such that the next segment initial point is in the slice $\hat{x}_2 = 0$, $\hat{x}_1 > 0$. Reconsider this as a sequence of infinitesimal time steps, each followed by an infinitesimal rotation such that the next segment initial point is in the slice $x_2 = 0$, $x_1 > 0$. Derive the corresponding $4d$ reduced state space ODE for the complex Lorenz flow.

10.32. **Accumulated phase shift:** Derive the $1d$ equation (10.50) for the accumulated phase shift θ associated with the 4-dimensional reduced state space ODE of exercise 10.31.

10.33. **The moving frame flow stays in the reduced state space:** Show that the flow (10.49) stays in a $(d-1)$-dimensional slice.

10.34. **Relative equilibrium TW_1 by the method of slices:** Determine numerically the complex Lorenz equations equilibrium TW_1 by the method of slices, template $\hat{x}'$ of your choice.

10.35. **State space reduction by a relative equilibrium TW_1 template:** Replace integration of the complex Lorenz equations by a sequence of short time steps, each followed by a rotation such that the next segment initial point is in the relative equilibrium TW_1 slice

$$(\hat{x} - \hat{x}_{TW_1}) \cdot t_{TW_1} = 0\,, \qquad t_{TW_1} = \mathbf{T}\hat{x}_{TW_1}\,, \tag{10.73}$$

where for any x, $\hat{x} = g(\theta) \cdot x$ is the rotation that lies in the slice. Check figure 10.12 by long-time integration of (10.49).

10.36. **Stability of a relative equilibrium in the reduced state space:** Find an expression for the stability matrix of the system at a relative equilibrium when a linear slice is used to reduce the symmetry of the flow.

10.37. **Stability of a relative periodic orbit in the reduced state space:** Find an expression for the Jacobian matrix (monodromy matrix) of a relative periodic orbit when a linear slice is used to reduce the dynamics of the flow.

References

[10.1] P. Cvitanović, R. L. Davidchack, and E. Siminos, On state space geometry of the Kuramoto-Sivashinsky flow in a periodic domain, `arXiv:0709.2944`; SIAM J. Appl. Dyn. Syst., to appear, 2009.

[10.2] M. Hamermesh, *Group Theory and Its Application to Physical Problems* (Dover, New York, 1962).

[10.3] R. Penrose. *The Road to Reality: A Complete Guide to the Laws of the Universe* (Knopf, New York 2005).

[10.4] G. W. Bluman and S. Kumei, *Symmetries and Differential Equations* (Springer, New York, 1989).

[10.5] M. Nakahara, *Geometry, Topology and Physics* (Inst. of Physics Publ., Bristol, 1990).

[10.6] E. Siminos, *Recurrent Spatio-temporal Structures in Presence of Continuous Symmetries*, Ph.D. thesis (Georgia Inst. of Tech. 2009); `ChaosBook.org/projects/theses.html`.

[10.7] E. Siminos and P. Cvitanović, Continuous symmetry reduction and return maps for high dimensional flows, Physica D (2010).

[10.8] M. Golubitsky and I. Stewart, *The Symmetry Perspective* (Birkhäuser, Boston, 2002).

[10.9] R. Hoyle, *Pattern Formation: An Introduction to Methods* (Cambridge Univ. Press, Cambridge, 2006).

[10.10] J. E. Marsden and T. S. Ratiu, *Introduction to Mechanics and Symmetry*, (Springer, New York 1999).

[10.11] P. J. Olver, *Classical Invariant Theory* (Cambridge Univ. Press, Cambridge, 1999).

[10.12] G. Bredon, *Introduction to Compact Transformation Groups* (Academic Press, New York, 1972).

[10.13] M. Krupa, Bifurcations of relative equilibria, SIAM J. Math. Anal. **21**, 1453 (1990).

[10.14] R. H. Cushman and L. M. Bates, *Global Aspects of Classical Integrable Systems*, p. 402 (Birkhäuser, Boston, 1997).

[10.15] J. G. Yoder, *Unrolling Time: Christiaan Huygens and the Mathematization of Nature* (Cambridge Univ. Press, Cambridge, 1988).

[10.16] C. Huygens, *L'Horloge à Pendule* (Swets & Zeitlinger, Amsterdam, 1673).

[10.17] F. Malige, P. Robutel, and J. Laskar, Partial reduction in the N-body planetary problem using the angular momentum integral, Celestial Mech. Dynam. Astronom. **84**, 283 (2002).

[10.18] A. Vierkandt, Über gleitende und rollende bewegung, Monatshefte für Math. und Phys. **III**, 31–54 (1892).

[10.19] A. M. Bloch, J. E. Marsden, and D. V. Zenkov, Nonholonomic dynamics, Notices of the AMS **52**, 324 (2005).

[10.20] A. Chenciner, A note by Poincaré, Regul. Chaotic Dyn. **10**, 119 (2005).

[10.21] H. Poincaré, Sur les solutions périodiques et le principe de moindre action, C. R. Acad. Sci. Paris **123**, 915 (1896).

[10.22] R. Broucke, On relative periodic solutions of the planar general three-body problem, Celestial Mech. Dynam. Astronom. **12**, 439 (1975).

[10.23] A. Chenciner and R. Montgomery, A remarkable solution of the 3-body problem in the case of equal masses, Ann. Math. **152**, 881 (2000).

[10.24] A. Chenciner, J. Gerver, R. Montgomery, and C. Simó, Simple choreographic motions of n-bodies: A preliminary study, in *Geometry, Mechanics and Dynamics*, edited by P. Newton, P. Holmes, and A. Weinstein, pp. 287–308 (Springer, New York 2002).

[10.25] C. McCord, J. Montaldi, M. Roberts, and L. Sbano, Relative periodic orbits of symmetric Lagrangian systems, in *Proceedings of "Equadiff 2003*, edited by F. Dumortier and et.al., pp. 482–493, 2004.

[10.26] S. Smale, Topology and mechanics, I., Inv. Math. **10**, 305 (1970).

[10.27] M. Field, Equivariant dynamical systems, Bull. Amer. Math. Soc. **76**, 1314 (1970).

[10.28] D. Ruelle, Bifurcations in presence of a symmetry group, Arch. Rational Mech. Anal. **51**, 136 (1973).

[10.29] R. Gilmore and C. Letellier, *The Symmetry of Chaos* (Oxford Univ. Press, Oxford, 2007).

[10.30] A. G. Vladimirov, V. Y. Toronov, and V. L. Derbov, The complex Lorenz model: Geometric structure, homoclinic bifurcation and one-dimensional map, Int. J. Bifur. Chaos **8**, 723 (1998).

[10.31] K. Gatermann, *Computer Algebra Methods for Equivariant Dynamical Systems* (Springer, New York, 2000).

[10.32] P. Chossat and R. Lauterbach, *Methods in Equivariant Bifurcations and Dynamical Systems* (World Scientific, Singapore, 2000).

[10.33] E. Cartan, La méthode du repère mobile, la théorie des groupes continus, et les espaces généralisés, Exposés de Géométrie **5** (1935).

[10.34] M. Fels and P. J. Olver, Moving coframes: I. A practical algorithm, Acta Appl. Math. **51**, 161 (1998).

[10.35] M. Fels and P. J. Olver, Moving coframes: II. Regularization and theoretical foundations, Acta Appl. Math. **55**, 127 (1999).

[10.36] V. I. Arnol'd, *Ordinary Differential Equations* (Springer, New York, 1992).

[10.37] D. V. Anosov and V. I. Arnol'd, *Dynamical systems I: Ordinary Differential Equations and Smooth Dynamical Systems* (Springer, 1988).

[10.38] V. I. Arnol'd, V. V. Kozlov, and A. I. Neishtadt, *Mathematical Aspects of Classical and Celestial Mechanics* (Springer, New York, 1988).

[10.39] C. W. Rowley and J. E. Marsden, Reconstruction equations and the Karhunen-Loéve expansion for systems with symmetry, Physica D **142**, 1 (2000).

[10.40] V. Guillemin and S. Sternberg, *Symplectic Techniques in Physics* (Cambridge Univ. Press, Cambridge, 1990).

[10.41] J. J. Duistermaat and J. A. C. Kolk, *Lie Groups* (Springer, New York, 2000).

[10.42] R. S. Palais, On the existence of slices for actions of non-compact Lie groups, Ann. Math. **73**, 295 (1961).

[10.43] G. D. Mostow, Equivariant embeddings in Euclidean space, Ann. Math. **65**, 432 (1957).

[10.44] A. N. Zaikin and A. M. Zhabotinsky, Concentration wave propagation in 2-dimensional liquid-phase self-oscillating system, Nature **225**, 535 (1970).

[10.45] A. T. Winfree, Scroll-shaped waves of chemical activity in 3 dimensions, Science **181**, 937 (1973).

[10.46] A. T. Winfree, *The Geometry of Biological Time* (Springer, New York, 1980).

[10.47] D. Barkley, M. Kness, and L. S. Tuckerman, Spiral wave dynamics in a simple model of excitable media: Transition from simple to compound rotation, Phys. Rev. A **42**, 2489 (1990).

[10.48] D. Barkley, Euclidean symmetry and the dynamics of rotating spiral waves, Phys. Rev. Lett. **72**, 164 (1994).

[10.49] B. Fiedler, B. Sandstede, A. Scheel, and C. Wulff, Bifurcation from relative equilibria of noncompact group actions: skew products, meanders, and drifts, Doc. Math. **141**, 479 (1996).

[10.50] B. Sandstede, A. Scheel, and C. Wulff, Dynamics of spiral waves on unbounded domains using center-manifold reductions, J. Diff. Eqn. **141**, 122 (1997).

[10.51] B. Sandstede, A. Scheel, and C. Wulff, Bifurcations and dynamics of spiral waves, J. Nonlinear Sci. **9**, 439 (1999).

[10.52] B. Fiedler and D. Turaev, Normal forms, resonances, and meandering tip motions near relative equilibria of Euclidean group actions, Arch. Rational Mech. Anal. **145**, 129 (1998).

[10.53] A. Mielke, *Hamiltonian and Lagrangian Flows on Center Manifolds* (Springer, New York, 1991).

[10.54] V. N. Biktashev, A. V. Holden, and E. V. Nikolaev, Spiral wave meander and symmetry of the plane, Int. J. Bifur. Chaos **6**, 2433 (1996).

[10.55] , J. F. Gibson, J. Halcrow and P. Cvitanović, *Equilibrium and traveling-wave solutions of plane Couette flow*, J. Fluid Mech. **638**, 243–266 (2009; `arXiv:0808.3375`.

[10.56] H. Wedin and R. R. Kerswell. Exact coherent structures in pipe flow. *J. Fluid Mech.*, 508:333–371, 2004.

[10.57] R. R. Kerswell. Recent progress in understanding the transition to turbulence in a pipe. *Nonlinearity*, 18:R17–R44, 2005.

[10.58] D. Rand, Dynamics and symmetry - predictions for modulated waves in rotating fluids, Arch. Rational Mech. Anal. **79**, 1 (1982).

[10.59] G. Haller and I. Mezić, Reduction of three-dimensional, volume-preserving flows with symmetry, Nonlinearity **11**, 319 (1998).

[10.60] J. E. Marsden and A. Weinstein, Reduction of symplectic manifolds with symmetry, Rep. Math. Phys. **5**, 121 (1974).

[10.61] F. Kirwan, The topology of reduced phase spaces of the motion of vortices on a sphere, Physica D **30**, 99 (1988).

[10.62] C. W. Rowley, I. G. Kevrekidis, J. E. Marsden, and K. Lust, Reduction and reconstruction for self-similar dynamical systems, Nonlinearity **16**, 1257 (2003).

[10.63] W.-J. Beyn and V. Thümmler, Freezing solutions of equivariant evolution equations, SIAM J. Appl. Dyn. Syst. **3**, 85 (2004).

[10.64] V. Thümmler, *Numerical Analysis of the Method of Freezing Traveling Waves*, PhD thesis, Bielefeld Univ., 2005.

[10.65] J. E. Marsden and T. S. Ratiu, *Introduction to Mechanics and Symmetry* (Springer, New York, 1994).

[10.66] V. Y. Toronov and V. L. Derbov, Geometric phases in lasers and liquid flows, Phys. Rev. E **49**, 1392 (1994).

[10.67] V. Y. Toronov and V. L. Derbov, Geometric-phase effects in laser dynamics, Phys. Rev. A **50**, 878 (1994).

[10.68] V. Y. Toronov and V. L. Derbov, Geometric phases in a ring laser, Quantum Electronics **27**, 644 (1997).

[10.69] C. Z. Ning and H. Haken, Phase anholonomy in dissipative optical-systems with periodic oscillations, Phys. Rev. A **43**, 6410 (1991).

[10.70] C. Z. Ning and H. Haken, An invariance property of the geometrical phase and its consequence in detuned lasers, Z. Phys. B **89**, 261 (1992).

[10.71] C. Z. Ning and H. Haken, Geometrical phase and amplitude accumulations in dissipative systems with cyclic attractors, Phys. Rev. Lett. **68**, 2109 (1992).

[10.72] G. Bluman, Connections between symmetries and conservation laws, SIGMA **1**, 011 (2005), `arXiv:math-ph/0511035`.

[10.73] G. W. Bluman and S. C. Anco, *Symmetry and Integration Methods for Differential Equations* (Springer, New York, 2002).

[10.74] H. J. Lipkin, *Lie Groups for Pedestrians* (North-Holland, Amsterdam, 1966).

[10.75] R. Gilmore, *Lie Groups, Physics, and Geometry* (Cambridge Univ. Press, Cambridge, 2008).

[10.76] J. D. Gibbon and M. J. McGuinness, The real and complex Lorenz equations in rotating fluids and lasers, Physica D **5**, 108 (1982).

[10.77] A. C. Fowler, J. D. Gibbon, and M. J. McGuinness, The complex Lorenz equations, Physica D **4**, 139 (1982).

[10.78] C. z. Ning and H. Haken, Detuned lasers and the complex Lorenz equations: Subcritical and supercritical Hopf bifurcations, Phys. Rev. **41**, 3826 (1990).

[10.79] A. Bakasov and N. Abraham, Laser second threshold: Its exact analytical dependence on detuning and relaxation rates, Phys. Rev. A **48** (1993).

[10.80] R. Wilczak, Reducing the state-space of the complex Lorenz flow, NSF REU summer 2009 project (U. of Chicago, 2009), `ChaosBook.org/projects/Wilczak/blog.pdf`, 2009.